598
2009

Berichte
zur Polar-
und Meeresforschung

Reports
on Polar and Marine Research

The Expedition of the Research Vessel "Pelagia" to the Natal Basin and the Mozambique Ridge in 2009 (Project AISTEK III)

Edited by
Wilfried Jokat
with contributions of the participants

HELMHOLTZ
GEMEINSCHAFT

ALFRED-WEGENER-INSTITUT FÜR
POLAR- UND MEERESFORSCHUNG
In der Helmholtz-Gemeinschaft
D-27570 BREMERHAVEN
Bundesrepublik Deutschland

ISSN 1866-3192

Hinweis

Die Berichte zur Polar- und Meeresforschung werden vom Alfred-Wegener-Institut für Polar-und Meeresforschung in Bremerhaven* in unregelmäßiger Abfolge herausgegeben.

Sie enthalten Beschreibungen und Ergebnisse der vom Institut (AWI) oder mit seiner Unterstützung durchgeführten Forschungsarbeiten in den Polargebieten und in den Meeren.

Es werden veröffentlicht:

— Expeditionsberichte (inkl. Stationslisten und Routenkarten)
— Expeditionsergebnisse (inkl. Dissertationen)
— wissenschaftliche Ergebnisse der Antarktis-Stationen und anderer Forschungs-Stationen des AWI
— Berichte wissenschaftlicher Tagungen

Die Beiträge geben nicht notwendigerweise die Auffassung des Instituts wieder.

Notice

The Reports on Polar and Marine Research are issued by the Alfred Wegener Institute for Polar and Marine Research in Bremerhaven*, Federal Republic of Germany. They appear in irregular intervals.

They contain descriptions and results of investigations in polar regions and in the seas either conducted by the Institute (AWI) or with its support.

The following items are published:

— expedition reports (incl. station lists and route maps)
— expedition results (incl. Ph.D. theses)
— scientific results of the Antarctic stations and of other AWI research stations
— reports on scientific meetings

The papers contained in the Reports do not necessarily reflect the opinion of the Institute.

The „Berichte zur Polar- und Meeresforschung"
continue the former „Berichte zur Polarforschung"

* Anschrift / Address
Alfred-Wegener-Institut
Für Polar- und Meeresforschung
D-27570 Bremerhaven
Germany
www.awi.de

Editor in charge:
Dr. Horst Bornemann

Assistant editor:
Birgit Chiaventone

Die "Berichte zur Polar- und Meeresforschung" (ISSN 1866-3192) werden ab 2008 ausschließlich als Open-Access-Publikation herausgegeben (URL: http://epic.awi.de).

Since 2008 the "Reports on Polar and Marine Research" (ISSN 1866-3192) are only available as web based open-access-publications (URL: http://epic.awi.de)

The Expedition of the Research Vessel "Pelagia" to the Natal Basin and the Mozambique Ridge in 2009 (Project AISTEK III)

Südöstlicher Atlantik und südwestlicher Indik:
Rekonstruktion der sedimentären und tektonischen Entwicklung seit der Kreide
AISTEK-III: Natal Becken und Mosambik Rücken

Southeastern Atlantic and southwestern Indian Ocean:
reconstruction of the sedimentary and tectonic development since the Cretaceous
AISTEK-III: Natal Basin and Mozambique Ridge

Edited by
Wilfried Jokat
with contributions of the participants

Please cite or link this publication using the identifier
hdl:10013/epic.33430 or http://hdl.handle.net/10013/epic.33430

ISSN 1866-3192

AISTEK III

Leg 64PE302 April 9th to May 6th, 2009

Leg 64PE306 May 7th to June 1st, 2009

Durban - Durban

Chief Scientist
Wilfried Jokat

Coordinator
Marieke Rietveld, NIOZ

Wilfried Jokat
Alfred-Wegener-Institut für Polar- und Meeresforschung
FB Geosystem
Am Alten Hafen 26
D-27568 Bremerhaven
Germany
Wilfried.Jokat@awi.de

BMBF Förderkennzeichen 03G0730A

CONTENTS

1. Summary

The expedition AISTEK III with RV *Pelagia* operated in the Natal Basin and the Mozambique Ridge off southern Africa. It was split for allowing refueling the vessel into two legs: 64PE305 – April 9th to May 6th, 2009 and 64PE306 – May 7th to June 1st, 2009. The harbor for both legs was Durban, RSA. The scientific goals were to acquire new geoscientific data in the above-mentioned areas to shed new light on the early seafloor spreading history during the Mesozoic Gondwana break-up. Thus, the main experiment was to systematically gather marine magnetic data to identify magnetic spreading anomalies. In general, the line spacing varied between 18 and 36 km, and had a N-S orientation. In the northern Natal Basin, additional E-W lines were acquired since the N-S line layout provided no unique pattern of spreading anomalies. The measurements were accomplished with a towed magnetic gradiometer system, consisting of two Overhauser sensors, and a ship-mounted fluxgate magnetometer.

In addition, gravity data were acquired with a LaCoste & Romberg S 56 gravimeter. Harbor measurements were taken four times in Durban. Furthermore, swath bathymetric data with a Simrad EM301 system and a 3.5 kHz sediment echosounder data were acquired along all tracks. Both systems are ship-mounted and were provided and prepared by NIOZ.

The most striking result of the cruise has been that the denser magnetic lines show the Mozambique Ridge having been formed at a mid-ocean ridge. Magnetic stripes can be identified in the data, which support this conclusion. Magnetic stripes in the southern Natal Basin are very subdued but visible and confirm more or less the old geodynamic models for this area. The northern Natal Basin shows are more complex magnetic pattern, but some trends are visible. A surprising result is that no pronounced magnetic anomaly marks the termination of continental/transitional crust in the area.

The bathymetry and the 3.5 kHz echosounder data show only little evidence of large current-controlled seafloor deposits. Most of the time, the seafloor was rather smooth, and the echosounder data had almost no penetration to allow the identification of channel-levee complexes. Future studies will compare these results with existing seismic data to make a final judgment. Dredging of shallow targets was attempted at two locations, but without any success. In total, three CTD casts were taken for the calibration of the Simrad EM 301 swath system. In general, the water velocity models were rather constant in the entire survey area.

During the two legs (29 days, 26 days) the ship sailed in total 19637 km (10603 nm) with a mean speed of 8-8.5 ktns/9-9.5 knts, respectively.

2. Zusammenfassung

Das AISTEK III Projekt hatte geophysikalische Messungen im Natal Becken und dem Mosambik Rücken vor dem südlichen Afrika zum Ziel. Die Messungen wurden mit dem holländischen Forschungsschiff FS *Pelagia* durchgeführt. Aus logistischen Gründen (Treibstoff, Proviant) wurde die Reise in zwei Abschnitte geteilt: 64PE305 – 9. April bis 6. Mai 2009, und 64PE306 – 7. Mai bis 1. Juni 2009. Für alle Zwischenstopps diente Durban (Rep. Südafrika) als Hafen.

Das Ziel des Vorhabens war es, mit Hilfe neuer geowissenschaftlicher Daten bessere Erkenntnisse über die frühe Entwicklungsgeschichte dieser Region (Meeresbodenspreizung) während des mesozoischen Aufbruchs von Gondwana zu gewinnen. Der Schwerpunkt der Arbeiten lag daher auf der Gewinnung neuer marin-magnetischer Daten, um magnetische Spreizungsanomalien in den untersuchten Regionen zu identifizieren. Der Linienabstand der einzelnen Profile variierte zwischen 18 und 36 km und die Profile hatten überwiegend eine N-S Orientierung. Im nördlichen Natal Becken wurden zusätzlich Ost-West Linien vermessen, um sicherzustellen, dass eine entsprechend orientierte Spreizungsachse nicht aufgrund des großen Linienabstandes übersehen wird. Die magnetischen Daten wurden mit einem geschleppten Gradiometersystem bestehend aus zwei Overhauser Sensoren und einem auf dem Schiff installierten Fluxgate Magnetometers erhoben.

Zusätzlich wurden Schweredaten mit einem LaCoste & Romberg S56 Gravimeter gemessen. Anschlusswerte wurden während der vier Aufenthalte in Durban bestimmt. Ferner wurden Fächersonardaten mit dem Simrad EM 301 und 3.5 kHz Sedimentecholotdaten entlang der gesamten Fahrtroute erhoben. Diese beiden Systeme wurden vom NIOZ zur Verfügung gestellt.

Eines der wichtigsten wissenschaftlichen Resultate dieser Expedition ist, dass der Mosambik Rücken an einem mittelozeanischen Rücken gebildet wurde. Magnetische Spreizungsanomalien wurden besser aufgelöst und bestätigen frühere Hypothesen hinsichtlich der geologischen Entwicklung des Mosambik-Rückens. Magnetische Spreizungsanomalien im südlichen Natal Becken sind weniger deutlich bzw. durch die Sedimentauflast stark abgedämpft. Die Interpretation bestätigt ältere geodynamische Interpretationen. Das nördliche Natal Becken hingegen zeigt komplexere magnetische Anomalien. Klare Trends, die auf Spreizungsanomalien hinweisen, sind nicht vorhanden. Spätere Analysen werden zeigen, ob sich schwächere Trends bestätigen oder nicht. Überraschenderweise zeigen die Daten keine klaren Potentialfeldanomalien, die auf die Kontinent-Ozean Grenze/Übergangszone im nördlichen Natal Becken hinweisen.

Die bathymetrischen Daten und auch die 3.5 kHz Sedimentecholotdaten zeigen kaum Hinweise auf Sedimentablagerungen, die durch Meeresbodenströmungen gebildet worden sind (sog. Driftsedimente). Der größte Teil des Meeresbodens ist sehr eben, und die 3.5 kHz Daten zeigen kaum Signale, die auf Driftsedimente hinweisen. Zukünftige Analysen werden diese Resultate mit vorhandenen seismischen Daten vergleichen, um eine abschließende Bewertung dieser ersten Beobachtung zu ermöglichen. Dredge-Stationen wurden an zwei Positionen ohne Erfolg durchgeführt. Insgesamt drei CTD Stationen zur Kalibrierung des Simrad EM301 System wurden eingemessen, um eine hochgenaue Tiefenberechnung zu ermöglichen. Das Geschwindigkeitsmodell für die Wassersäule war in der gesamten Region sehr konstant, so dass diese wenigen CTD Messungen ausreichten, um gute Tiefendaten zu erhalten.

Während dieser zwei Fahrtabschnitte (29 und 26 Tage) fuhr das Schiff insgesamt 19637 km (10603 SM) mit einer jeweils mittleren Geschwindigkeit von 8-8.5 ktn bzw. 9-9.5 ktn.

3. Fahrtverlauf / Itinerary

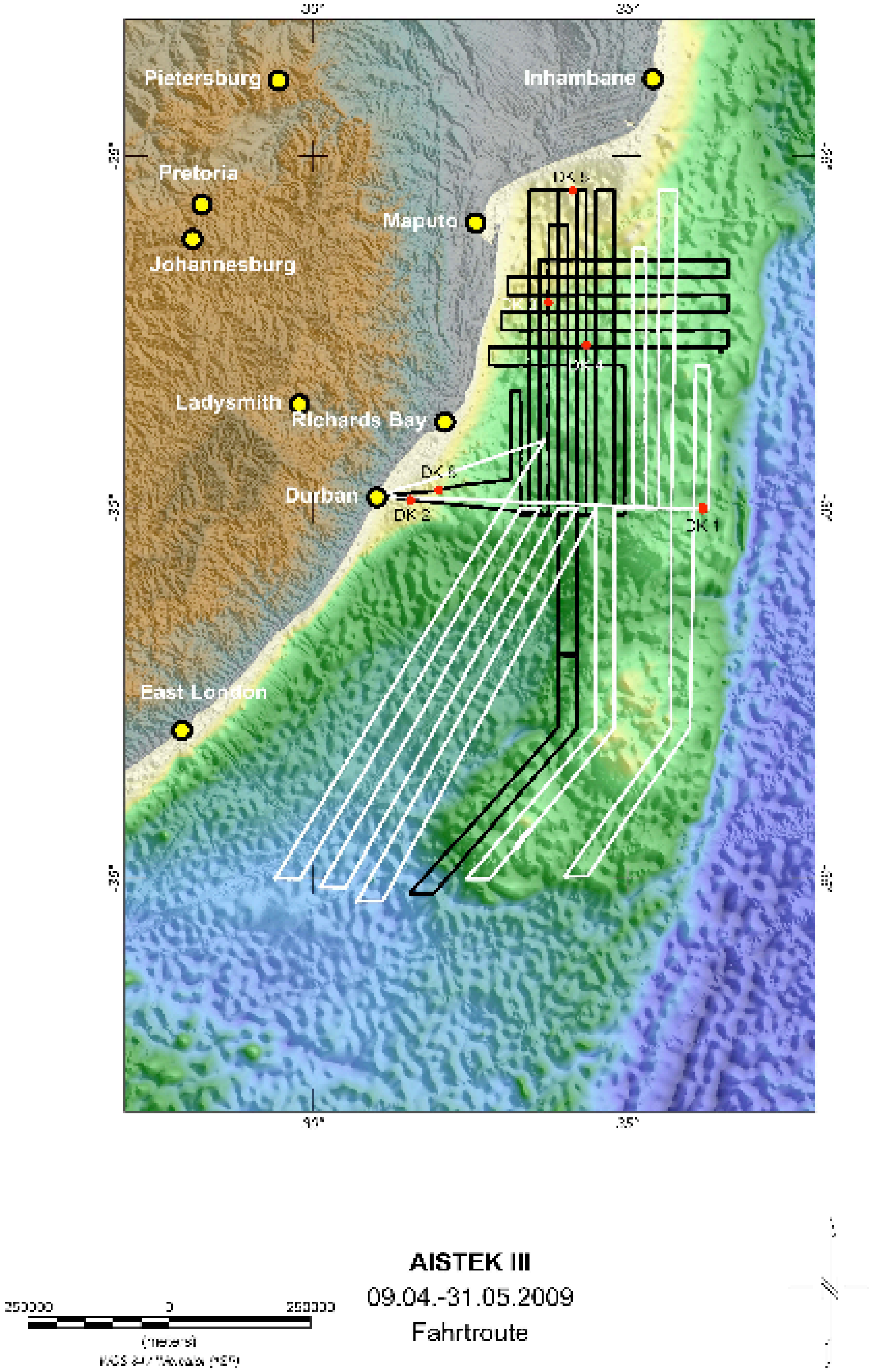

Fig. 1: Cruise tracks of RV Pelagia for the AISTEK III Project.
White Lines: leg 1: 64PE305, Black Lines: leg 2 - 64PE306. The red dots labeled with DK indicate the locations of the calibration circles for the ship mounted fluxgate three-component magnetometer.

4. Introduction

Wilfried Jokat
Alfred Wegener Institute, Bremerhaven, Germany

Reconstructing the continent configuration of the past presents particular problems as soon as one tries to explain the very early movements of the continents. Often, marine magnetic anomalies, which are formed at very young mid-ocean ridges at the rift-drift transition of a break-up process, are not well developed. The fact that the ship track based database is rarely dense enough to resolve the more complex magnetic pattern of this time period is another shortcoming. For the AISTEK III project, thus, the major scientific objective was to resolve details on the early spreading history of the Mozambique plains and the Natal Basin in comparison to the Mozambique Ridge. From the existing data, the transition of the oceanic crust in the southern Natal Basin to whatever type of crust comprising the basement of the northern Natal Basin is completely unknown. A similar interpretation status is found for the Mozambique Ridge. Rock samples collected over more than two decades provided mixed results for the origin of the ridge. Mid-ocean ridge basalts as well as continental rocks were dredged. In the absence of any modern deep seismic sounding data set in the strike of the Mozambique Ridge, most geophysical data favor an oceanic origin of the ridge. If the Mozambique Ridge formed at a spreading centre it should host magnetic stripes, which can be measured by a towed magnetometer system. However, no unique data set had been available so far to support one or the other hypothesis. What was the status of knowledge before the cruise started?

A deep seismic line at the southern end of the Mozambique Ridge acquired during the AISTEK I expedition in 2005 clearly supports that this part is of oceanic origin. This interpretation is strengthened by mid-ocean ridge basalt dredged in the vicinity during the AISTEK II expedition during the same season. Magnetic measurements across the Mozambique Ridge during the AISTEK II (2005) campaign further support this view. Highly variable magnetic anomalies with varying polarity, which might be caused by Mesozoic magnetic reversals, were recorded. However, the data set was not sufficient enough to undoubtedly prove the oceanic origin.

The AISTEK III expedition, thus, aimed to close the gaps of the previous two expeditions. Marine magnetic data were systematically acquired across the ridge as well as in the southern and northern Natal basins to supplement the existing information, in order to allow an enhanced reconstruction for this area of early Gondwana break-up.

5. Bathymetry

Ralf Krocker, Sarah Reinshagen, Daniel Damaske
Alfred Wegener Institute, Bremerhaven, Germany

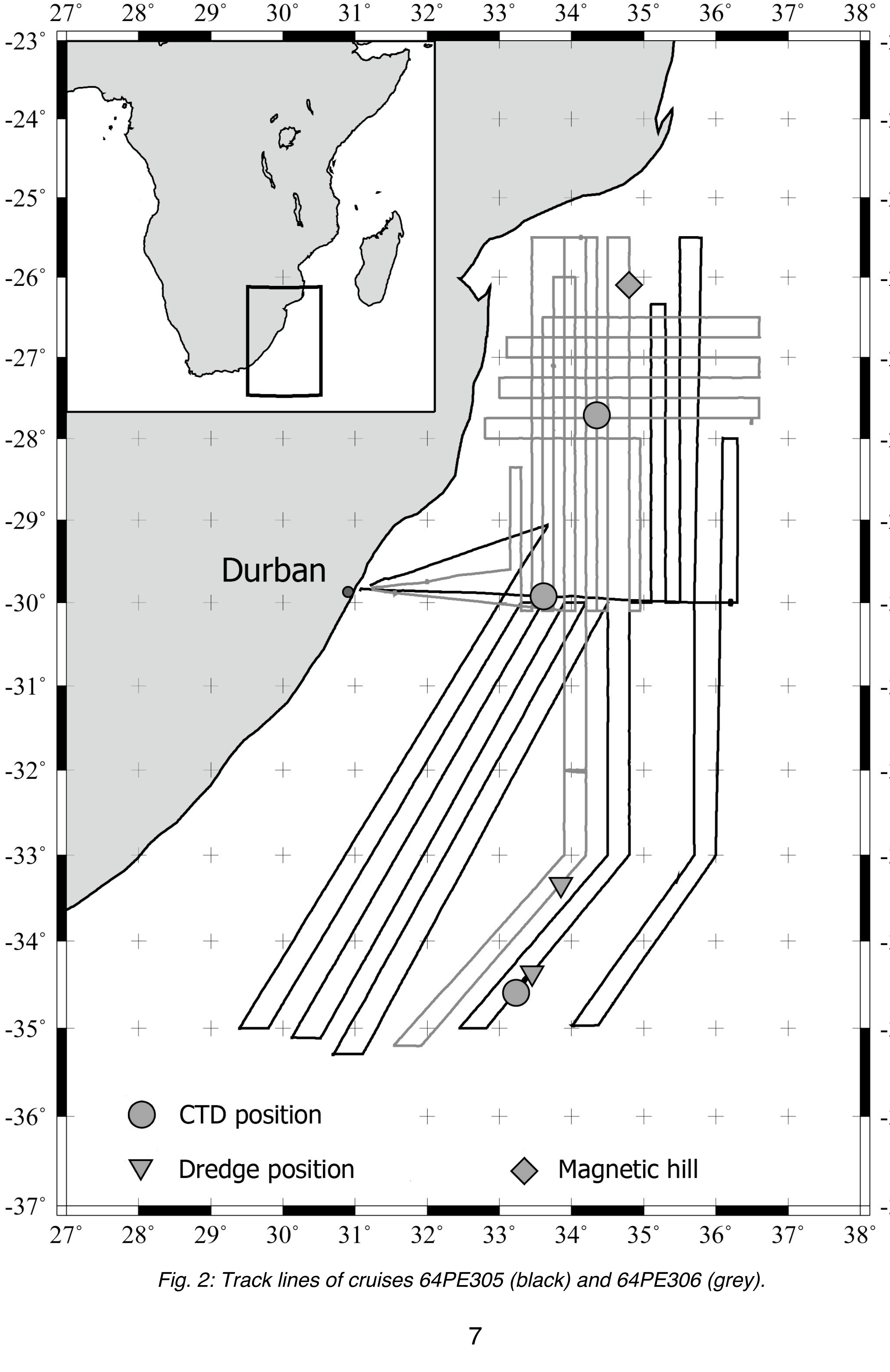

Fig. 2: Track lines of cruises 64PE305 (black) and 64PE306 (grey).

5.1 Summary

The swath sonar system was operated during the entire cruise without any failure. During 53 days of data sampling, data loss due to system errors amounts to less than one hour. The track length amounts to 10,598 nautical miles (19,627 km), whereas 5,404 nm (10,008 km) have been sailed on leg 64PE305 and 5,194 nm (9,619 km) on leg 64PE306. 17,765,455 pings were measured, split-up into 4,053,827,795 beams. In total, an area of approx. 57,923 km was covered with bathymetry. 2409 files of Simrad raw data format (*.all) in a total size of 31 GB were recorded. The track lines of these cruises are shown in figure 2. CTD profiles needed for depth calculation have been measured at three positions, as shown in figure 2.

5.2 Measuring the sound speed in water

The physical parameters of seawater within the water column were acquired by performing CTD measurements (Conductivity, Temperature, Depth). The depth component, however, is not measured directly but instead is being derived from the pressure of the water column. The measured conductivity and temperature parameters are also relevant for the pressure to depth conversion, as they allow the determination of the sea water density.

A further parameter is the geographic latitude, as this allows the varying magnitude of acceleration due to the gravity to be estimated. This acceleration determines the weight of any given mass of seawater, and therefore contributes to accurate depth determination for each pressure measurement.

Accurate CTD data are essential for the post-processing of multibeam data. Thus, variations of the sound velocity with depth must be known for the slant sonar beam refraction correction and for the depth determination. They can be calculated from CTD data. Due to the regional and local variations of the physical parameters, it is indispensable to input new sound velocity profiles (SVP) from actual CTD casts along Swath Echosounder survey lines.

5.3 Data Acquisition and Processing

The CTD on board R.V. *Pelagia* was developed by Sea-Bird Electonics Inc. (SBE), based on three different components: the underwater unit *(SEA-BIRD CTD-Underwaterunit 9plus*), a deck unit *(SEA-BIRD Model 11plus)* and an acquisition computer (PC). CTD measurements were acquired three times during the survey period. Figure 3 shows the workflow of CTD data from the measurement to the import into the Simrad *Seafloor Information System* (SIS).
The CTD underwater unit is deployed in sea water and sends the data continuously via cable to the deck unit. The acquisition computer running *Seasave Win32 version 5.37d* logs data acquired via the deck unit.

The acquired data was processed using *SBE Data Processing, Version 5.35.* The data processing properties are as follows:

- Calculate the derived parameters (depth in meters and sound velocity by using *Chen-Millero* formula)
- Group data into one meter bins
- Extract data from downcast only
- Convert the binary data to an ASCII-file
-

The CTD data is converted to mimic an *AML* sound velocity file output, using *SvpProcessing Version 1.1b* programmed by Alexey Andreev and installed on board R.V. *Pelagia*.

The final output data is transferred into (SIS) and thinned using the integrated tool *SVP Editor*. The sound speed profile is then ready for implementation. Table 1 and figure 3 show CTD statistics and graphical plots, respectively.

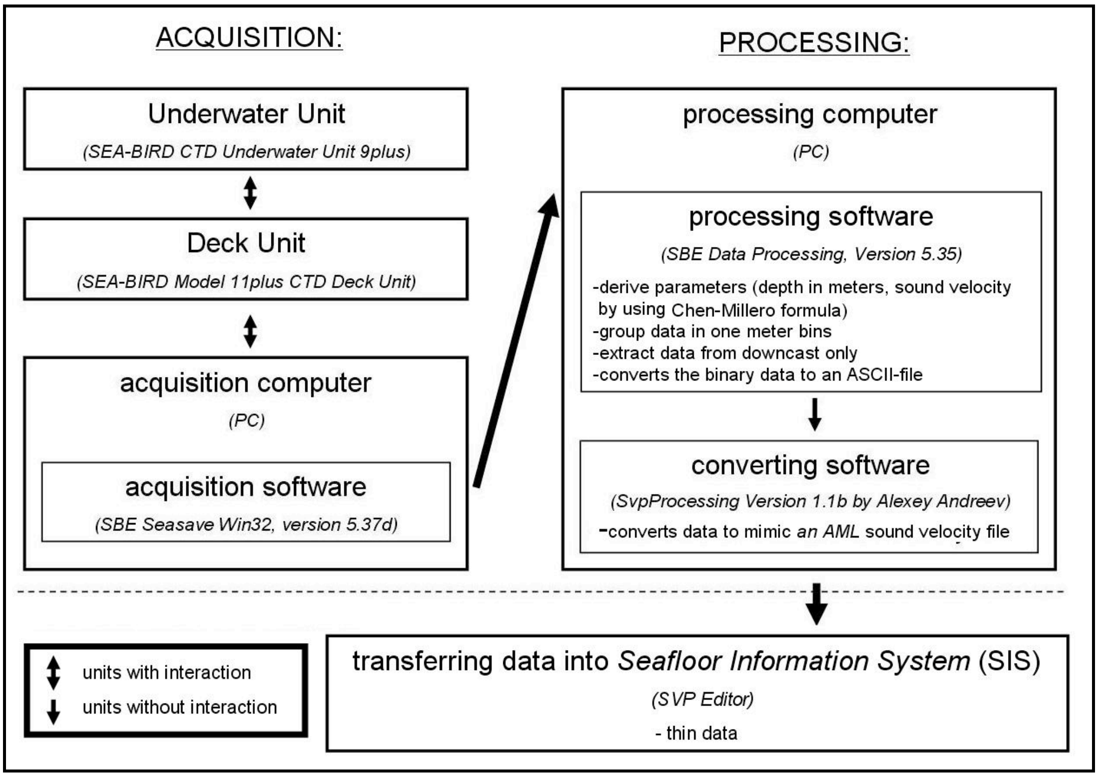

Fig. 3: CTD – workflow process on board R.V. Pelagia

Table 1: Statistics of the CTD measurements

Name of CTD file	Date UTC Time	Longitude	Latitude	Depth [m]	Name of converted file for SIS-System
dsoundvelprofile 1.cnv	10.04.2009 08:08	33°36'34''	-29°55'36''	2717	soundvelprofile1_thinned.asvp
dsoundvelprofile 2.cnv	22.04.2009 17:22	33°13'52''	-34°35'40''	2383	soundvelprofile2_thinned.asvp
dsoundvelprofile 3.cnv	27.05.2009 18:08	34°20'58''	-27°43'04''	1435	soundvelprofile3_thinned.asvp

In the northern part of the survey area, some refraction errors (more or less uncertainties) were detected during data editing. They may have been caused by variations in the water conditions due to fresh water currents from the nearby river orifices. Because of the unknown current flows, locations for addition CTD profile measurements were not defined. The establishment of several random distributed CTD measurements covering the whole area would have taken too much time and, therefore, were not conducted. Due to the small amount of refraction errors and its local limitations, this seemed to be acceptable.

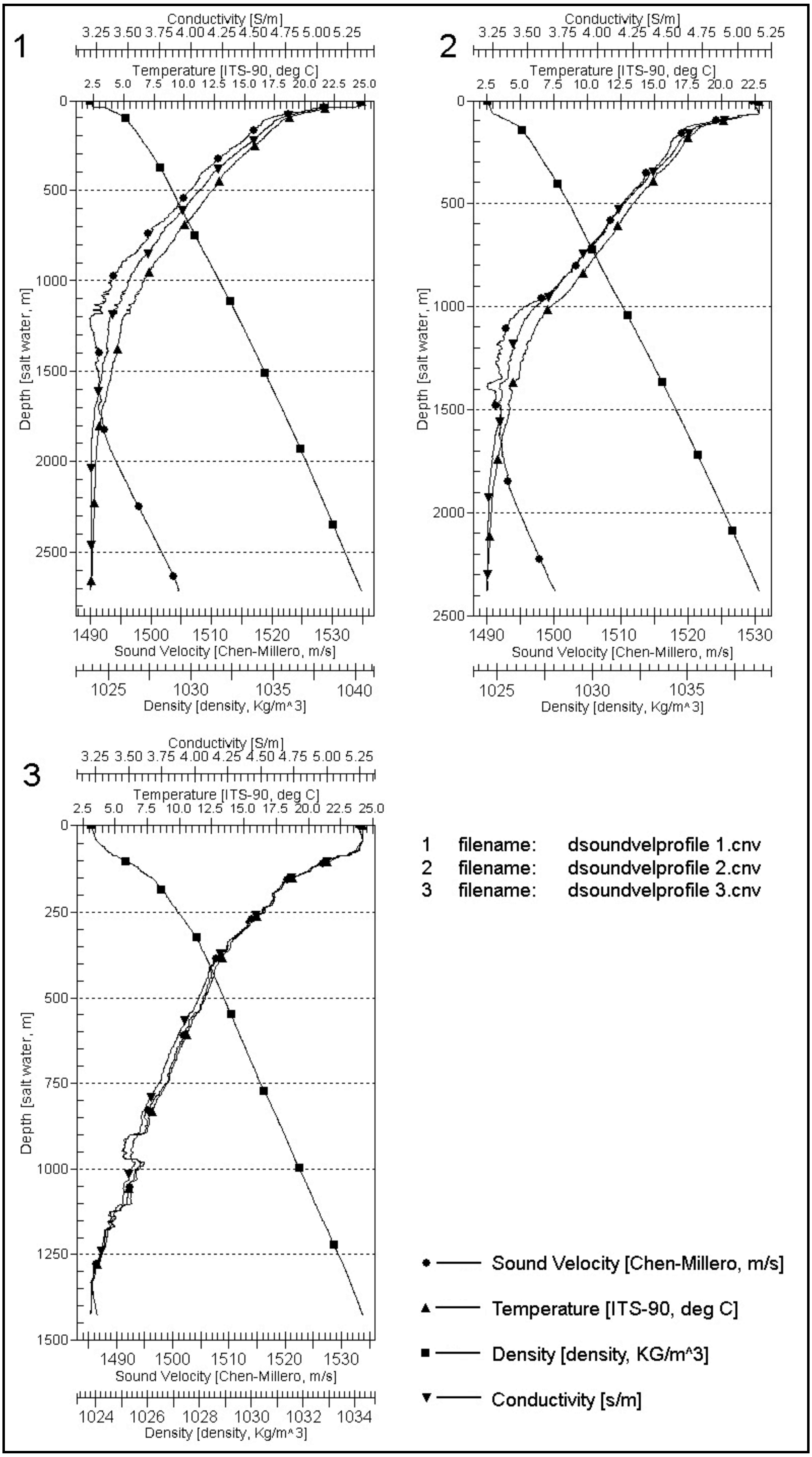

Fig. 4: Graphs of conductivity, temperature, density and sound velocity of the CTD profile measurements.

The sound velocity at the transducer is an important and sensitive parameter for depth calculation. For that reason, a sensor for measuring this parameter was installed at the ship's keel. Due to a bug in the SIS data acquisition software, the measured sound speed at the keel could not be used. The actual value was measured and displayed correctly, but seemed not to be applied properly as the source for depth calculation and was shown/dispayed in this environment to be 0. Thus, as source for the sound velocity at the keel only the measured CTD data were used. The measurements between the two sensors differ by less than 2m/s, which is negligible.

5.4 Swath sonar system description

Since the Kongsberg Simrad EM 302 was used the first time in a scientific marine geophysical project lead by AWI, a detailed description of the system and its operation is given. The following is derived from the Product Description from Kongsberg Simrad system.

The Kongsberg Simrad EM 302 Multibeam Echo Sounder is a deep water swath system, which is capable to map most part of the world's ocean. All necessary sensor interfaces, data displays for quality control and sensor calibration, seabed visualization, and data logging are part of the system. Furthermore, the EM 302 has an integrated acoustical seabed imaging capability (sidescan).

The operating Frequency is 30 kHz with an angular coverage sector of up to 150° with a resulting maximum swath width on a flat bottom of up to 5.5 times the water depth. The system transmits 288 beams per ping. The angular coverage sector and beam pointing angles may be set to vary automatically with depth and noise according to achievable coverage. This maximizes the number of usable beams.

The transmitted fan is split into several individual sectors with independent active steering depending on the roll, pitch and yaw of the vessel. This permits to concentrate all soundings on a "best fit" base to a sector perpendicular to the survey line, thus ensuring a uniform sampling of the bottom, and 100% coverage.

System characteristics

The Kongsberg Simrad EM 302 Multibeam Echo Sounder consists of the following units:

- Transmit transducer array
- Receive transducer array
- Transceiver Unit
- Preamplifier Unit (only if sub-bottom profiler is connected)
- Operator Station

A complete mapping system will also include the following additional units:

- Vessel motion sensor(s)
- Heading sensor
- Positioning system(s)
- Sound speed sensor(s)
- Post-processing system

Transceiver Unit:

The Transceiver Unit of the EM 302 contains electronics and processors for beam-forming, bottom detection, and control of all parameters with respect to gain, ping rate and transmit angles. It has serial interfaces for all time-critical external sensors such as vessel attitude (roll, pitch, heading and heave), vessel position and external clock. The Transceiver Unit is installed in a wall mounted cabinet with integrated shock and vibration absorbers. The same cabinet is used for all combinations of beam-widths.

Operator Station:

The Seafloor Information System (SIS) allows setting the EM 302 installation and runtime parameters, data logging and running self-test on the system without restrictions.
The SIS software also includes functionality for survey planning, 2D and 3D geographical display of the survey results, seabed image and water column displays, plus real-time data filter algorithms.

5.5 Swath sonar system operation

The EM 302 multibeam echo sounder is controlled from the HWS (Hydrographic work station) using a standard graphical user interface. The software, Seafloor Information System (SIS), is running on the Microsoft Windows XP operating system, which is installed on the HWS.

The system does not require elaborate operator intervention during normal operation, but tracks the bottom automatically. Before the operation is started, the necessary external sensors, namely positioning and vessel motion sensors, are connected and calibration procedures followed in order to define the system and sensor installation parameters. The system includes an automatic calibration facility.

SIS provides the graphical displays required for real-time control of the EM 302, such as:

- Cross-track depth profiles
- Beam intensities and quality measures
- Time series display of beam samples and sensor values
- 3D waterfall display
- Sound speed profile display and editor

Data Logging

It is of utmost importance to ensure that all survey related data are logged in a safe way. The data are always stored on disk, and displayed on the screen after having reread the data. This way, the operator has control on the storage status, and can identify any malfunction of the storage/disc system very efficiently.

The logged data sets include the following information

- Raw sensor data
- Beam ranges and beam pointing angles
- Depth datagrams
- Seabed image data
- System parameter settings
- Optional raw data (hydrophone or beam-formed)

The Simrad System is started using the EM Systems Remote Control. First, the Sound Velocity Sensor, and after that the Multibeam button has to be switched on. After a while, a message is shown in the Windows task panel showing/displaying the system is running.

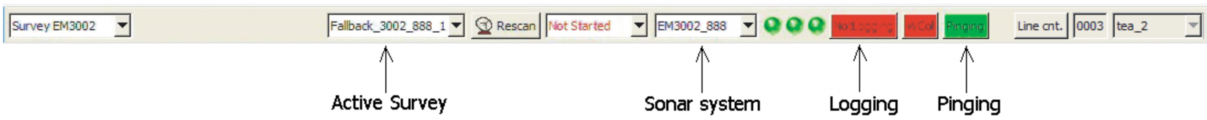

Fig. 5: SIS control panel for survey settings and sonar control.

At the beginning of a cruise, a new survey project has to be created. The system is creating a new folder on the storage device using the name of the survey project where the bathymetric raw data will be recorded in the proprietary binary Simrad-format for multibeam raw data (extension: *.all).
In order to create a new survey, the button 'New Survey' in the dropdown list from one of the control windows must be selected. In the newly opened window the name of the survey must be typed in and be confirmed by OK. The next step is to select the created survey in the combo-box as active survey. Finally, the Simrad System must be selected in the combo-box (here: EM3002_888) to replace default value 'NONE'.
After setting the parameters in the 'Runtime parameters' window (see below), the system can be switched on. This will be done by selecting the button 'Start Pinging'. The quality of measured depths can be interpreted within the several control windows. The red button 'Logging' is pressed to start the data logging. After all, the buttons 'Pinging' and 'Logging' are underlain in green.

Adjusting the Runtime parameters

The operator may set several parameters for sound transmission and receiving, as well as for online filtering. The settings can be adjusted in the control window 'Runtime Parameters' (Fig. 6). Due to changes in seafloor topography and weather conditions, these parameters have to be updated constantly. One can choose the automatic mode for updating some parameters, but the manual adjustment by an experienced operator yields qualitatively and quantitatively better results.

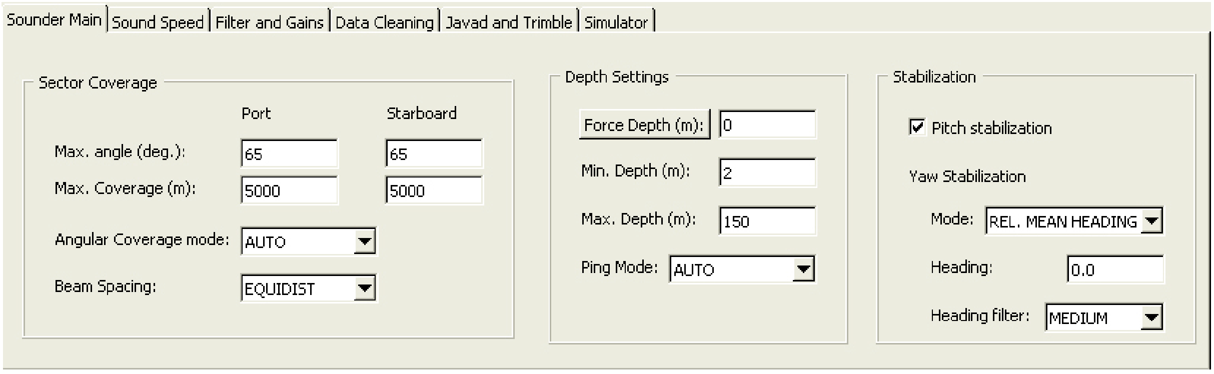

Fig. 6: SIS control window displaying runtime parameters.

In order to change the swath angle of the transmission signal, a value in the field next to '*Max. Angle (deg.)'* can be selected. There is one field for Port and one for Starboard site. The parameter '*Max. Coverage (m)'* can also be defined for both sites with different values.

For real time filtering, the '*Depth Settings'* can be used. Bad weather conditions or deep seafloor disables the multibeam system to automatically detect the depth of the seafloor. The values '*Min. Depth (m)'* and '*Max. Depth (m)'* can be pre-selected to provide the system with a valid depth range. A stronger constraint is to press the button '*Force Depth (m)',* to pre-set the actual depth of seafloor. The '*Ping Mode'* can manually be adjusted to the water depth. Due to strongly changing environmental conditions, it is impossible to give a rule of thumb on how to set the parameters as a function of depth. The operator has to test and find out the optimal settings.

During data acquisition and an additional calibration survey, the ship's speed was detected as an important environmental parameter for signal-to-noise ratio. As a consequence, during survey with ship's speed of 9 knots, the maximal possible swath width were decreased significantly.

The settings for online filtering can be found on tab 'filter and gains'. The following settings were chosen for this survey:

Spike Filter Strength: MEDIUM
Range Gate: SMALL

All check-boxes except the one for '*Slope'* and '*Sector Tracking*' were unselected.

The settings for data cleaning can be found on the corresponding tab. The slider indicating the degree of real time data cleaning was set to 'none'.

5.6 Data cleaning

The main idea is to record the entire data during acquisition and remove implausible depths in post processing for better control and with more sensitively chosen settings. Reasons for erroneous depths can be:

Roll or pitch error, slant range refraction error, transducer orientation error, ship's position error, gyro or heading error, heave error, omega and tunnel effect, interferences due to ship's noise, interferences from other hydroacoustic sensors, erroneous refraction correction, different backscattering from the sea floor, penetration of the nadir beam into the sea floor.

As a matter of fact, automatic algorithms cannot be used to sufficiently detect errors and filter the data as precise as an editing operator can do. For this reason, the data were cleaned manually by using the software system Caris HIPS.
In theory, errors can be separated into three groups: rough, systematic and random errors. In principal, only rough errors are subject of manual data cleaning. 69,394,158 of 4,053,827,795 beams (1.8 %) were marked as rough errors, and excluded for further processing.

Systematic errors, sometimes caused by a wrong SVP or biased in the attitude system, are corrected during post processing applying the corresponding algorithms, if available. For example: In the northern part of our working area, the used SVP was not correct and had to be replaced by the values from the third CTD profile, which was taken at the end of the cruise.

5.7 Data examples

The figures 7-9 show the two dredge locations, as well as the profile across the magnetic hill. Grids are calculated from edited bathymetry with grid spacing of 0.01' x 0.01' (~ 15.2 x 18.5 meter) using GMT bicubic spline algorithm.

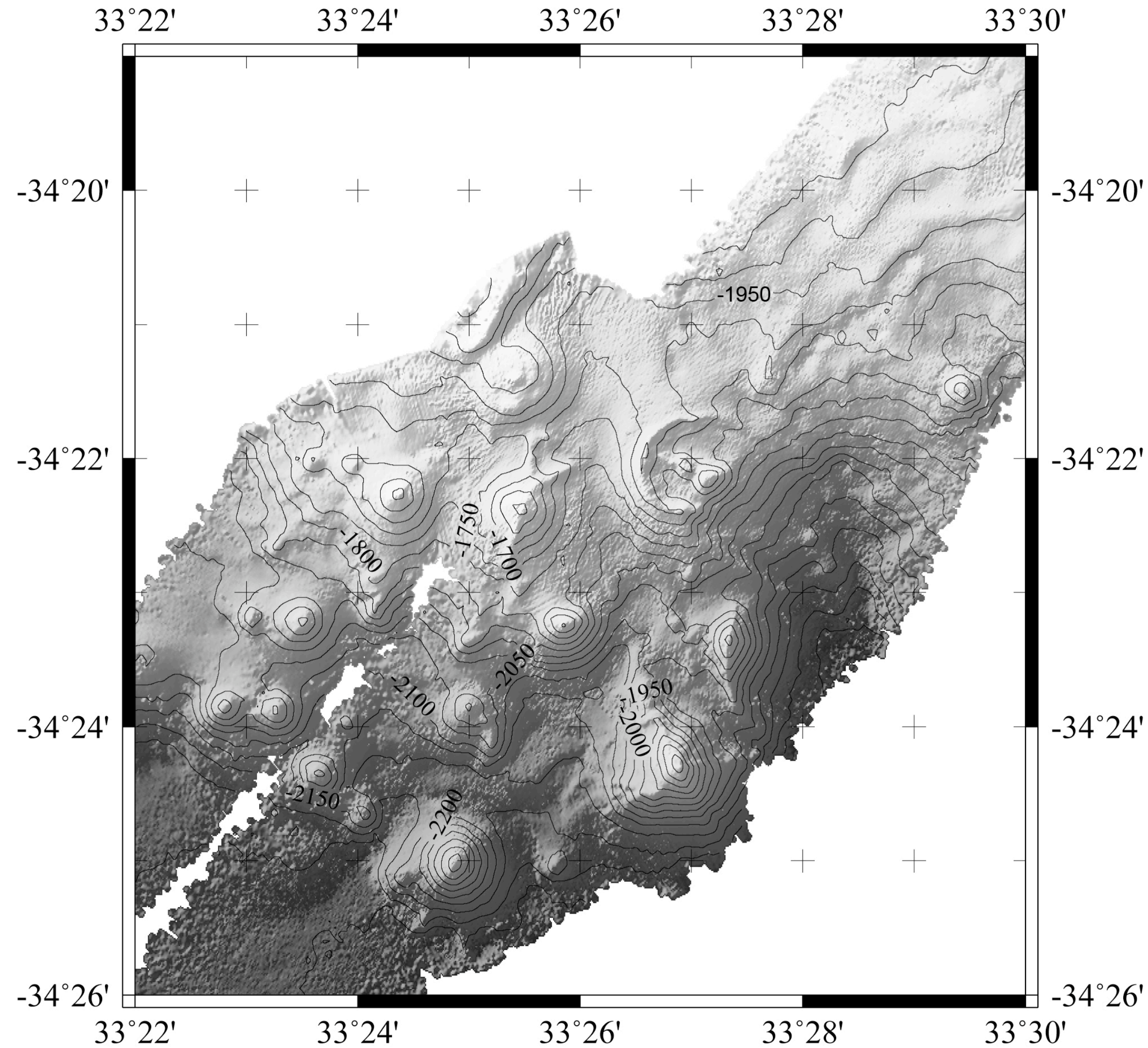

Fig. 7: The crater centred in 34°22'S / 33°27'E at depth of approx. 1700 meter was dredged on its western rim. Contour line interval is 50 meter.

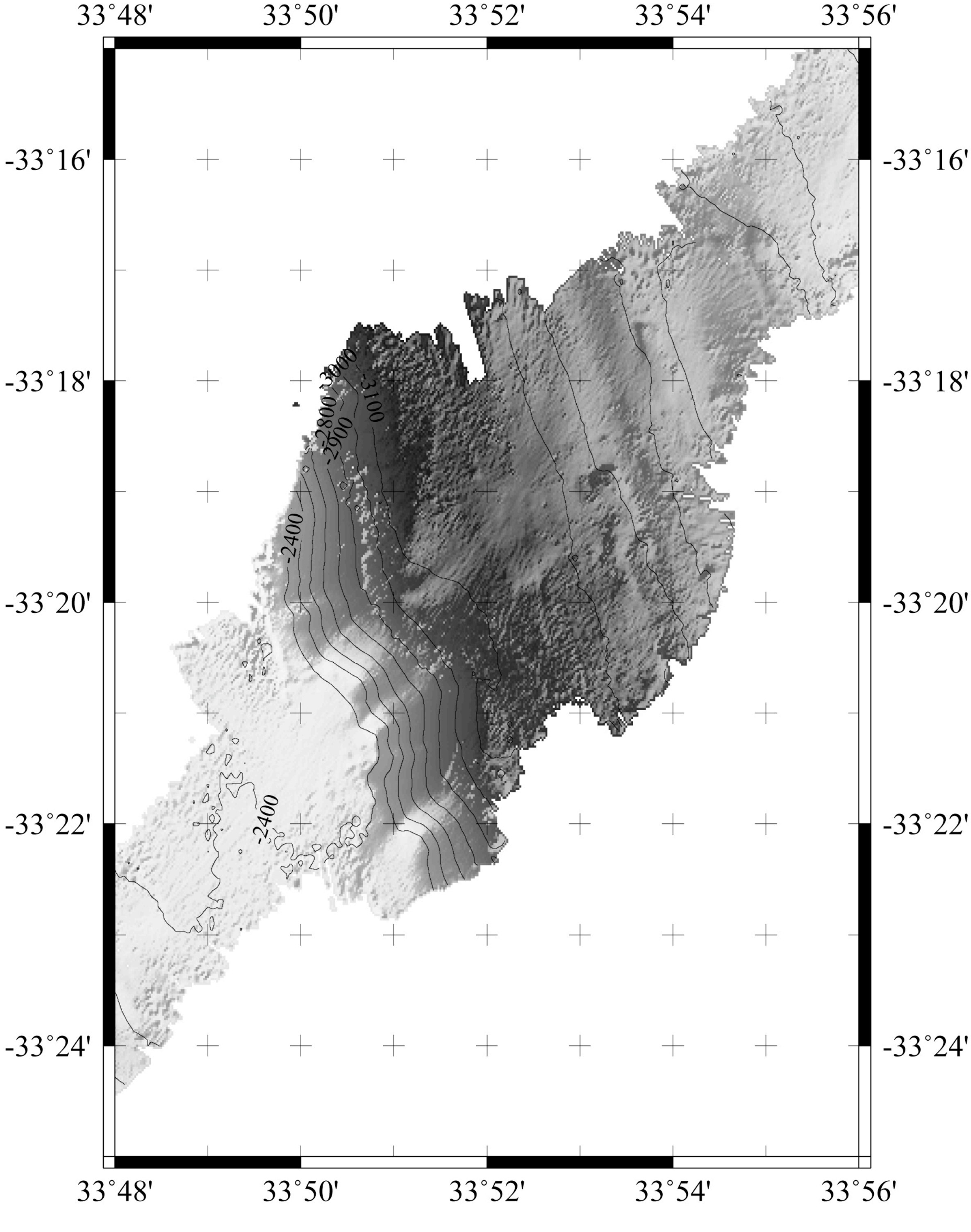

Fig. 8: The dredged slope ranges from 3150 meter in the centre of the channel to 2380 meter to the top. The distance between these points amounts to approx. 4 km. Contour interval is 100 meter.

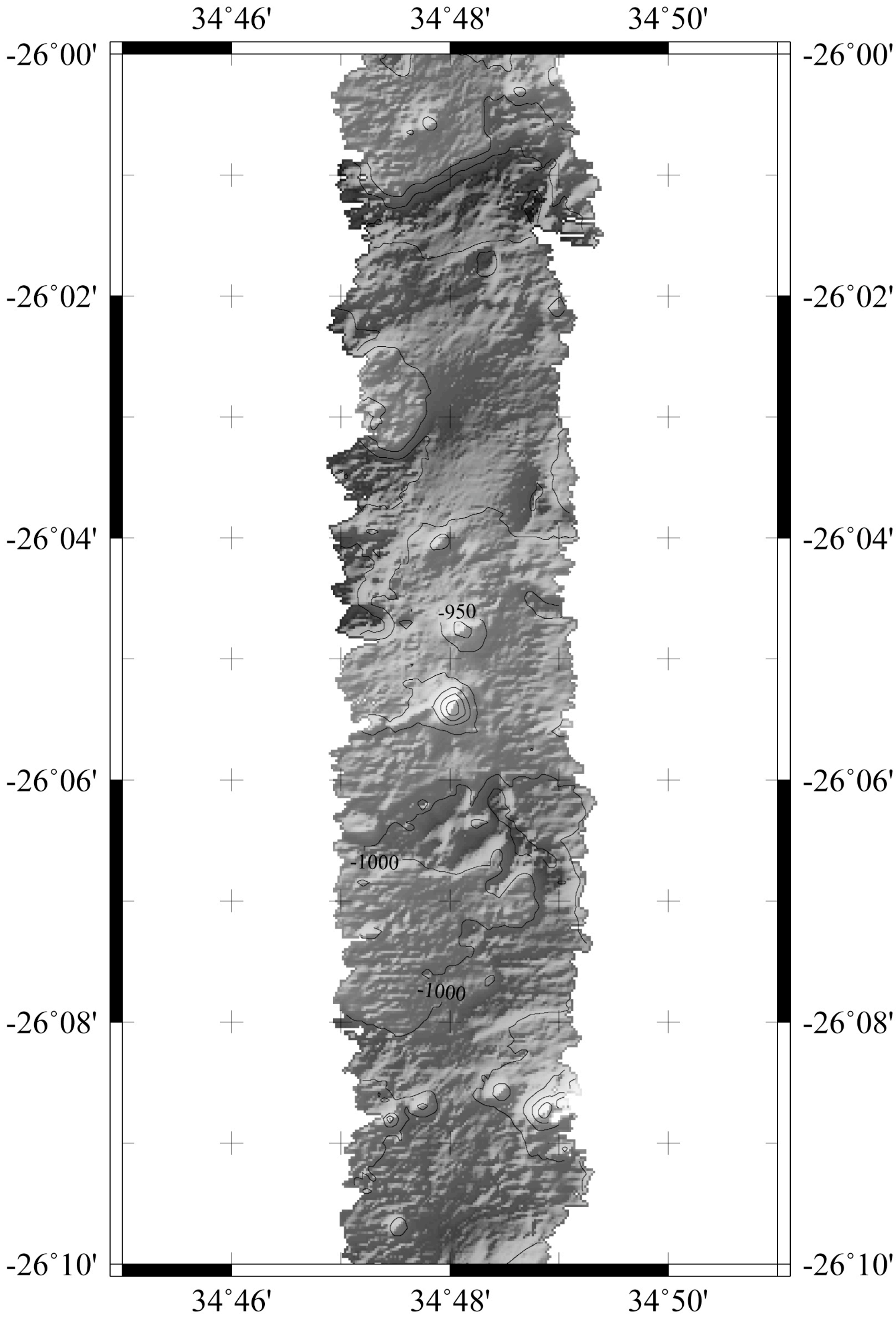

Fig. 9: Topography of the 'Magnetic hill' and the adjacent area. The peak has a height of 758 meter, whereas the surroundings amount to approx. 970 meter. The swath width amounts to ca. 3700 meter. Contour interval is 50 meter

5.8 Data delivery

At the end of the cruise, the collected multibeam raw data were handed over to an observer from the Petroleum Agency South Africa. The data will also be delivered to the Federal Maritime and Hydrographic Agency (Bundesamt für Seeschifffahrt und Hydrographie – BSH). The bathymetry will be used for new compilations of Nautical Charts in this region. The data cover Plotting Sheets 373 and 403 of the 'General Bathymetric Chart of the Ocean' (GEBCO), which are also defined as map sheets 1.16 and 1.19 in the 'International Bathymetric Chart of the West Indian Ocean' – IBCWIO.

The data will also be published for scientific use. Edited multibeam data, grids and maps as well as CTD profiles will be available in the future on 'Publishing Network for Geoscientific and Environmental Data' – PANGAEA (www.pangaea.de).

6. Potential Field measurements

W. Jokat[1)], C. Kopsch[1)], V. Leinweber[1)], M. Ickrath[1)], T. Hanyu[2)]

[1)] Alfred Wegener Institute, Bremerhaven, Germany
[2)] NIPR, Tokyo, Japan

6.1 Magnetic Gradiometer measurements

To measure the magnetic field, a SeaSpy™ gradiometer, manufactured by Marine Magnetics Corp., was used. The gradiometer consisted of two independent Overhauser magnetometer, which were towed 300 m behind the ship with a spacing of 100 m. Each sensor measures simultaneously the total intensity of the earth magnetic field with an absolute accuracy of 0.1 nT without drift (specifications of the system). The horizontal gradient of the field can be obtained by subtracting the two values from each other, and dividing the obtained difference by the distance between the sensors. Assuming that the time variations of the earth magnetic field are spatially constant over the distance of the two sensors, one can get the total magnetic field (apart from a constant value) through integration of the gradients over the distance of the ship track.

The data acquisition was performed with a Laptop, which received the position information from an extra installed GPS system (Fig. 10).

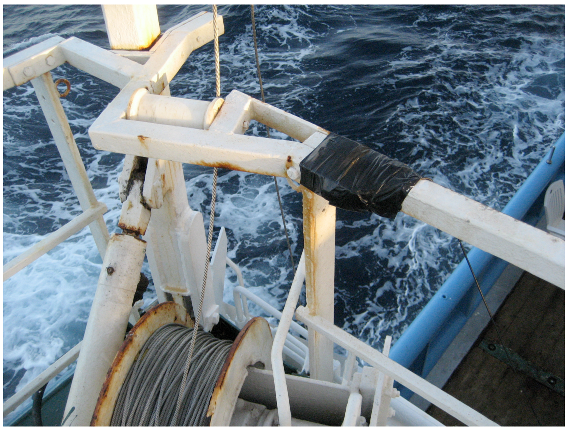

Fig. 10 above: GPS-antenna used for gradiometer system. Below: gradiometer sensor

Because of irregular excursions and spikes of the received coordinates by the magnetometer system, the ships' navigation data as used for the bathymetric SIMRAD system was stored additionally.

The general sailing speed was between 8 and 10 knots. The ship's speed of 10 knots and a measuring rate of 5s led to a sampling interval of roughly 25 m.
In the beginning of the cruise, we used a sampling rate of 1s for the data acquisition. Unfortunately, problems with the data acquisition system arose, and the system failed approximately every other day. One reason appeared to be insufficient grounding, and the system ran more stable after grounding the connection cable to the ship. Nevertheless, sometimes the system got hung up. We first switched the measuring rate to 3s, later to 5s, to assure a more stable data acquisition.

On May 17th, the acquisition laptop delivered by GSE rentals crashed with core errors. Thus, we had to replace the computer by one of our Toshiba toughbooks, which ran stable until the end of the cruise. On May 21st, we experienced another system crash. While getting the gradiometer back on the ship, we recognized that rear sensor towed a long-line as used to catch sharks. The rear sensor was damaged yet still working fine. Nevertheless, the reason for the problems seemed to be the winch, which was not transmitting the signal anymore. We exchanged the winch with the spare hand winch with an unarmored 200 m long cable. For weight reasons, we decided to use only the rear sensor for the last part of the cruise. From this moment on, no gradient measurements were possible. The magnetic data are generally of excellent quality.

First trials to integrate the gradient led to reasonable results concerning the shape of the obtained anomalies, but showed strong trends in the resulting total magnetic field. These can probably be explained by oblique measurements because of offsets of the sensor system in vertical direction to the ships track due to water currents.

6.2 Magnetic base station

The main reason to use a gradiometer system is to acquire data, which are free of diurnal variations and disturbances of the earth magnetic field because of solar activity. For control purposes and to have a backup system, in the event that one magnetic gradiometer sensor failed, we installed a magnetic base station in Durban, which was recording the earth's magnetic field during the entire cruise.
The base station - a GSM-19 Overhauser magnetometer – was installed in the garden of the cruise-participating scientist Mike Watkeys in Durban. To protect the equipment from "animal attacks", the sensor-bearing rod was protected by a non-metallic fence, and the cable from the sensor to the acquisition unit was surrounded by tubes and dug into the ground.

The sensor was driven by a regular power supply in the small garden house. The data acquisition unit was located inside. The GPS antenna was fixed on the gutter, as one can see on picture 11 just above the window.

Fig. 11a + b: Magnetic base station at Durban,
Start of measurement: 08.04.2009, 18:06:42 UTC
End of measurement: 31.05.2009, 13:35:32 UTC

6.3 Gravity measurements

During the entire cruise we conducted gravity measurements, using a LaCoste & Romberg S56 sea gravity meter. This gravity meter is a high-damped and astatized version of the normal L&R land gravity meter and is mounted on a stabilizing platform (Fig. 12).

Simply put, the sensor consists of a mass that is attached to movable beam. A zero-length-spring holds the sensor free in place.

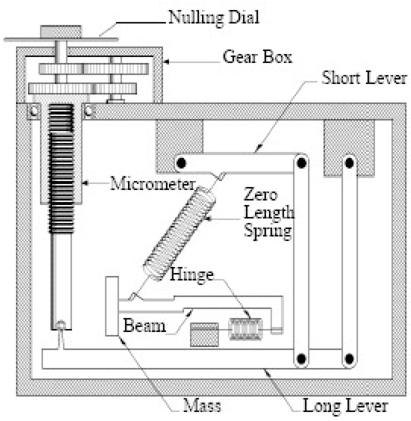

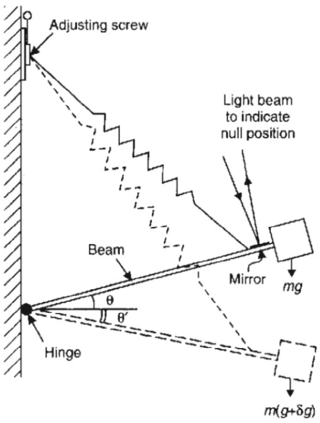

Fig. 12 a + b: Principle drawings of the gravity meter, the movable beam and the zero-length spring

On a moving ship, the roll and pitch movements of the vessel produce an acceleration on the meter beam, which heavily disturbs the measurement of the gravity acceleration of the earth. To deal with this fundamental problem at sea, a pair of gyros and accelormeters control torque motors stabilize the long and short axes of the gravity meter to hold it in a horizontal plane. A special algorithm between these three units keeps the platform stable like a dampened pendulum. The large vertical acceleration of the ship is damped by air dampers.

Measuring the position of the beam as well as its velocity and its acceleration, one can calculate the gravity. The acceleration term of the equation can be neglected in the case of a highly damped beam. If the gravity sensor has a very high sensitivity, the position term can be neglected also. Both was the case for the used gravity meter. Thus, the resulting equation is:

$$\mathbf{g = S + kB' + CC}$$

(g ... gravity meter reading, S ... spring tension, k... sensor specific constant,
B' ... beam velocity, CC ... cross coupling corrections)

The gravity meter was installed onboard the ship, roughly following the checklist printed in the Appendix A.2.

The system was installed in the chemical lab room, on the starboard side of the ship (Fig. 13). The position of the sensor in relation to the master point of the ship has been:

x = + 3,50 m (positive: to starboard)
y = + 5,57 m (positive: forward)
z = - 4,01 m (positive: downward)

Fig 13 a + b: S56 Sea gravimeter installed on RV Pelagia

A K-Check (see A.5 and A.6)was performed with the following result:

Spring Tension: 9349,0	Total Correction: -0,1
Spring Tension: 9379,0	Total Correction: -30,0
Spring Tension: 9319,0	Total Correction: 30.0

During the cruise, the system was running autonomously, but checked regularly. The data were continuously stored by a laptop. The gravity meter was not connected to a GPS-antenna, the system time of the PC was stored with the gravity values. Therefore, it was necessary to make manual comparisons of the GPS-time with the system time to be able to assign the positions in a post-processing process and to correct this assignment for the drift of the laptop's system clock.

A gravity meter like the one used measures only differences in gravity between two stations, not the absolute gravity. Therefore, every survey should be related to the datum and the scale of a reference system. The International Gravity Standardization Net IGSN71 stations distributed worldwide are the commonly used reference system. To link the ship measurements to this network, we used a portable L&R land gravity meter.

Measurements at an IGSN-point and on the pier next to the ship allow transforming the simultaneous measurements of the sea gravity meter to the IGSN71.

These measurements were repeated during the stay in Durban between the two cruise legs and at the end of the cruise. Another important objective of these measurements is to provide an estimate for the instrument drift.

6.4 Gravity harbor measurements

Tie measurements were conducted on the beginning of the cruise (April 9^{th} 2009, marked with "A"), between the first and the second cruise leg (May $06^{th}/07^{th}$ 2009, marked with "B") and, finally, at the end of the cruise (May 31^{st} 2009, marked with "C"). As a reference point, the ISGN71-point in the Durban Durmarine Building was used:

Port Captain's office, Durmarine Building
Longitude: 31°2.13'E
Latitude: 29°52.05'S
979348.66 mGal
(Bureau Gravimetrique International, BGI, Toulouse, France)

Construction work was being conducted in the Durmarine building. Therefore, access was complicated. To avoid difficulties for future campaigns, we took a measurement in front of the monument "Lady in white" located in front of the building (see pictures below). This point was used as reference point for the measurements in the end of the cruise.

At the end of the cruise, the measurement near Poller 80 from April 9^{th} 2009 was repeated as control point. The absolute gravity value, calculated of the reference value from DULW C differed from the absolute gravity value at the beginning of the cruise by 0.24 mGal.

Table 2: Harbor values measured in Durban, RSA

Station	Date	Time	L&R gravity [mGal]	abs. gravity [mGal]
DURM A	09.04.2009	11:00	2997,36	979348.66
P80 A	09.04.2009	09:36	2996,30	979347,60
SHIP A	09.04.2009	08:16	2996,20	979347,50
SHIP B1	06.05.2009	05:10	3000,17	979351,88
DURM B	07.05.2009	05:10	2996,95	979348,66
DULW B	07.05.2009	05:22	2997,02	979348,73
SHIP B2	07.05.2009	06:35	3000,26	979351,97
SHIP C	31.05.2009	12:41	2995,55	979347,43
P80 C	31.05.2009	13:00	2995,48	979347,36 (979347,60)
DULW C	31.05.2009	14:29	2996,85	979348,73

Table 3: Readings at the beginning of the cruise

09.04.2009 Durban Durmarine Building Port Captain's Office, under construction				Resulting Gravity [mGal]: 2997,36 DURM A		
Time (UTC)	Counter reading [CU]	Kind of measurement	Feedback [mV]	Feedback [mGal]	Counter reading [mGal]	Total gravity [mGal]
10:53	2933,68	manual	0,000	0,000	2997,41	2997,41
10:57	2933,00	Feedback	0,606	0,609	2996,71	2997,32
10:58	2932,50	Feedback	1,114	1,119	2996,20	2997,32
11:00	2934,00	Feedback	-0,347	-0,349	2997,73	2997,38
11:01	2934,50	Feedback	-0,838	-0,842	2998,24	2997,40
11:02	2934,75	Feedback	-1,125	-1,130	2998,50	2997,37
11:04	2933,50	Feedback	0,121	0,122	2997,22	2997,34
11:08	2933,61	manual	0,000	0,000	2997,33	2997,33

Figure 14: Gravity point in the Durmarine Building

Table 3 a +b +c: Gravity reading close to RV Pelagia

09.04.2009 Durban port next to the ship on pollar 80 (white)				Resulting Gravity [mGal]: 2996,30 P80 A		
Time (UTC)	Counter reading [CU]	Kind of measurement	Feedback [mV]	Feedback [mGal]	Counter reading [mGal]	Total gravity [mGal]
9:22	2932,63	manual	0,000	0,000	2996,33	2996,33
9:25	2933,00	Feedback	-0,372	-0,374	2996,71	2996,34
9:38	2933,00	Feedback	-0,438	-0,440	2996,71	2996,27
9:39	2933,50	Feedback	-0,885	-0,889	2997,22	2996,33
9:41	2932,50	Feedback	0,051	0,051	2996,20	2996,25

09.04.2009 Durban Harbor pier Maiden Wharf next to *Pelagia* at position of gravity meter S56				Resulting Gravity [mGal]: 2996,32		
Time (UTC)	Counter reading [CU]	Kind of measurement	Feedback [mV]	Feedback [mGal]	Counter reading [mGal]	Total gravity [mGal]
11:57	2932,59	manual	0,000	0,000	2996,29	2996,29
11:58	2932,50	Feedback	0,083	0,083	2996,20	2996,28
12:00	2932,00	Feedback	0,598	0,601	2995,69	2996,29
12:02	2933,00	Feedback	-0,370	-0,372	2996,71	2996,34
12:03	2933,50	Feedback	-0,835	-0,839	2997,22	2996,38
12:08	2932,25	Feedback	0,345	0,347	2995,94	2996,29
12:09	2932,75	Feedback	-0,130	-0,131	2996,45	2996,32
12:11	2932,64	manual	0,000	0,000	2996,34	2996,34

09.04.2009 Durban Harbor pier Maiden Wharf, repeated measurement next to *Pelagia* at position of gravity meter S56				Resulting Gravity SHIP [mGal]: 2996,20 A		
Time (UTC)	Counter reading [CU]	Kind of measurement	Feedback [mV]	Feedback [mGal]	Counter reading [mGal]	Total gravity [mGal]
16:45	2932,43	manual	0,000	0,000	2996,13	2996,13
16:46	2932,00	Feedback	0,459	0,461	2995,69	2996,15
16:47	2931,75	Feedback	0,763	0,767	2995,43	2996,20
16:48	2931,50	Feedback	0,946	0,950	2995,18	2996,13
16:48	2932,50	Feedback	0,020	0,020	2996,20	2996,22
16:49	2932,75	Feedback	-0,224	-0,225	2996,45	2996,23
16:50	2933,25	Feedback	-0,708	-0,711	2996,97	2996,25
16:54	2932,39	manual	0,000	0,000	2996,09	2996,09

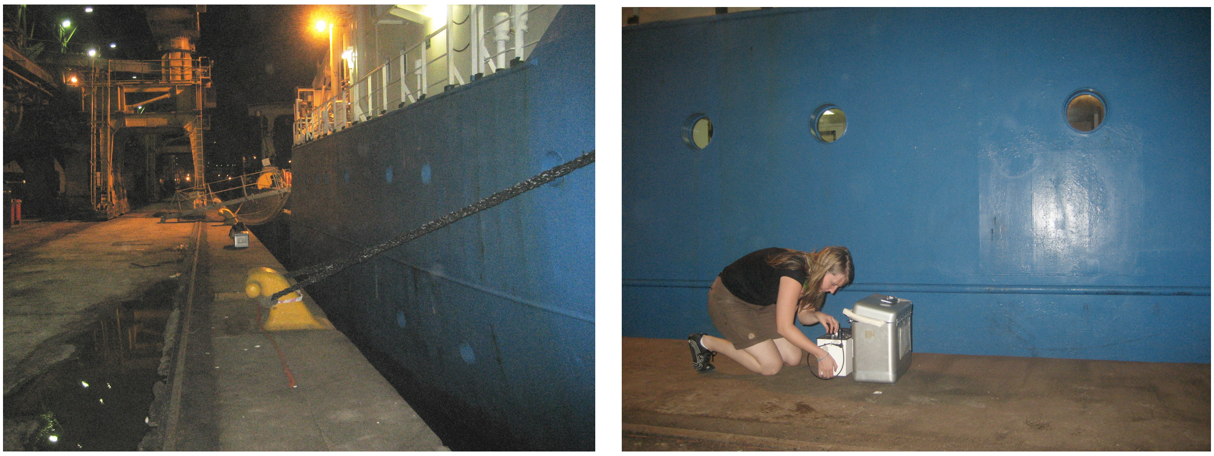

Fig. 14: Gravity readings in Durban close to RV Pelagia

Table 4: Gravity readings in Durban between leg 1 and 2.

06.05.2009 Durban port, next to ***Pelagia***, 1 m right of pollar 129 (viewing to the ship)				<u>Resulting Gravity [mGal]:</u>	3000,17	SHIP B1
Time (UTC)	**Counter reading [CU]**	**Kind of measurement**	**Feedback [mV]**	**Feedback [mGal]**	**Counter reading [mGal]**	**Total gravity [mGal]**
8:11	2936,44	manual	0,000	0,000	3000,22	3000,22
8:12	2936,00	Feedback	0,372	0,374	2999,78	3000,15
8:13	2935,75	Feedback	0,653	0,656	2999,52	3000,18
8:15	2935,50	Feedback	0,840	0,844	2999,27	3000,11
8:16	2936,25	Feedback	0,164	0,165	3000,03	3000,20
8:17	2936,50	Feedback	-0,129	-0,130	3000,29	3000,16
8:18	2936,75	Feedback	-0,332	-0,334	3000,54	3000,21
8:19	2937,00	Feedback	-0,578	-0,581	3000,80	3000,22
8:20	2936,39	manual	0,000	0,000	3000,17	3000,17

Fig. 15 a + b: Gravity measurements alongside RV Pelagia at the stop between legs 1+2.

07.05.2009 Durban Durmarine Building, Port Captain’s Office, under construction Longitude: 31°02,102783 E Latitude: 29°52',094015 S				Resulting Gravity [mGal]: 2996,95		DURM B
Time (UTC)	Counter reading [CU]	Kind of measurement	Feedback [mV]	Feedback [mGal]	Counter reading [mGal]	Total gravity [mGal]
5:05	2933,21	manual	0,000	0,000	2996,92	2996,92
5:06	2933,00	Feedback	0,227	-0,228	2996,71	2996,94
5:08	2932,75	Feedback	0,457	-0,459	2996,45	2996,91
5:09	2932,50	Feedback	0,706	-0,709	2996,20	2996,91
5:10	2933,25	Feedback	-0,007	0,007	2996,97	2996,96
5:11	2933,50	Feedback	-0,249	0,250	2997,22	2996,97
5:12	2933,75	Feedback	-0,499	0,501	2997,48	2996,98
5:12	2934,00	Feedback	-0,738	0,741	2997,73	2996,99
5:14	2933,22	manual	0,000	0,000	2996,93	2996,93

07.05.2009 Durban Durmarine Building, in front of the statue " Durban`s Lady in White" Longitude: 31° 02',09568 E Latitude: 29° 52',100736 S				Resulting Gravity [mGal]: 2997,02		DULW B
Time (UTC)	Counter reading [CU]	Kind of measurement	Feedback [mV]	Feedback [mGal]	Counter reading [mGal]	Total gravity [mGal]
5:19	2933,31	manual	0,000	0,000	2997,03	2997,03
5:19	2933,25	Feedback	0,029	0,029	2996,97	2996,99
5:20	2933,00	Feedback	0,272	0,273	2996,71	2996,98
5:21	2932,75	Feedback	0,513	0,515	2996,45	2996,97
5:22	2933,50	Feedback	-0,170	-0,171	2997,22	2997,05
5:23	2933,75	Feedback	-0,413	-0,415	2997,48	2997,06
5:24	2934,00	Feedback	-0,661	-0,664	2997,73	2997,07
5:26	2933,31	manual	0,000	0,000	2997,02	2997,02

07.05.2009 Durban port, next to Pelagia, repeated measurement 1 m right of pollar 129 (viewing facing the ship)				Resulting Gravity [mGal]: 3000,26		SHIP B2
Time (UTC)	Counter reading [CU]	Kind of measurement	Feedback [mV]	Feedback [mGal]	Counter reading [mGal]	Total gravity [mGal]
6:30	2936,44	manual	0,000	0,000	3000,23	3000,23
6:32	2936,00	Feedback	0,443	0,445	2999,78	3000,22
6:33	2936,25	Feedback	0,227	0,228	3000,03	3000,26
6:35	2936,50	Feedback	0,064	0,064	3000,29	3000,35
6:36	2936,75	Feedback	-0,313	-0,314	3000,54	3000,23
6:37	2937,00	Feedback	-0,510	-0,512	3000,80	3000,29
6:39	2935,75	Feedback	0,700	0,703	2999,52	3000,22
6:40	2936,43	manual	0,000	0,000	3000,22	3000,22

Table 5: Gravity measurements in Durban at the stop between legs 1+2.

Fig. 16: Gravity point in the Durmarine Building

Table 6 a: Gravity readings at the end of the cruise at different locations in Durban

31.05.2009 Durban port, pier Maiden Wharf 1m right of Pollar 80 (viewing in water direction), same point as 06.04.				Resulting Gravity [mGal]:		2995,48 P80 C
Time (UTC)	Counter reading [CU]	Kind of measurement	Feedback [mV]	Feedback [mGal]	Counter reading [mGal]	Total gravity [mGal]
12:57	2931,79	manual	0,000	0,000	2995,47	2995,47
12:58	2932,00		-0,210	-0,211	2995,69	2995,48
12:58	2932,25		-0,437	-0,439	2995,94	2995,50
12:59	2932,50		-0,672	-0,675	2996,20	2995,52
13:00	2931,75		0,032	0,032	2995,43	2995,46
13:01	2931,25		0,524	0,526	2994,92	2995,45
13:02	2931,00		0,773	0,777	2994,67	2995,44
13:03	2931,81	manual	0,000	0,000	2995,49	2995,49

Table 6 b: Gravity readings at the end of the cruise at different locations in Durban

31.05.2009 Durban Durmarine Building in front of statue " Durban`s Lady in White" Longitude: 31° 02',0910 E Latitude: 29° 52',0962 S				Resulting Gravity [mGal]:	2996,85	DULWC
Time (UTC)	Counter reading [CU]	Kind of measurement	Feedback [mV]	Feedback [mGal]	Counter reading [mGal]	Total gravity [mGal]
14:24:36	2933,12	manual	0,000	0,000	2996,83	2996,83
14:26:19	2933,00		0,140	0,141	2996,71	2996,85
14:27:12	2932,75		0,364	0,366	2996,45	2996,82
14:28:07	2932,50		0,600	0,603	2996,20	2996,80
14:28:53	2932,25		0,846	0,850	2995,94	2996,79
14:30:09	2933,25		-0,055	-0,055	2996,97	2996,91
14:31:14	2933,50		-0,309	-0,310	2997,22	2996,91
14:32:05	2933,16	manual	0,000	0,000	2996,87	2996,87

Fig. 17 a + b: Gravity points just in front of the Durmarine Building at the "Lady in white" monument

7. First results from the interpretation of the magnetic gradiometer data

Wilfried Jokat
Alfred Wegener Institute, Bremerhaven, Germany

The potential field data acquired in the research area have a high quality. Since we lost time because of the limited ship speed of an average of 8-9 ktns instead of 10 ktns, some regions could not be investigated in as much detail, as appropriate to geological complexity. E.g., the transition between the southern Natal Basin and the Mozambique Ridge could only be surveyed with a line spacing of 18 NM. The acquired data show that a spacing of 5-10 NM would be appropriate to map the complex transition zone. However, investigating the entire proposed research area, the ship being significant slower as previously planned, meant that we had to shorten the program, in this case to widen the line spacing. The results can be summarized for each of the three areas:

Southern Natal Basin (SNB)

The magnetic stripes previously are confirmed. Much to our surprise, most of the magnetic M-series are negative and subdued because of the large sediment thickness. Chron M4, however, could be identified with great confidence on all new lines. Its geographical location is in excellent correlation with the old magnetic data. The position of chron M0 is not that clear from our data. Here, a careful analysis is needed either to confirm or to revise its position.

Northern Natal Basin (NNB)

Just north of 30°S in the Natal Basin, the magnetic basement structures become more complex. This is confirmed by the few old single channel seismic lines, which show several plateaus. In general, the magnetic anomalies become stronger towards the north. Some structures are highly magnetized, which is reflected in their high magnetic gradient and amplitudes of well above 500 nT. Since the N-S lines in the NNB did not show clear trends, we decided to supplement the network by some E-W lines in order to avoid overseeing spreading anomalies running parallel to the coast of southern Africa. However, no such magnetic stripes were found in the data.
The few clear trends indicate that the strike direction from the SNB might continue at least partly into the NNB. Extensive volcanism obviously destroyed and/or biased the correlation of the magnetic anomalies or the sea floor spreading was less good structured during this break-up phase. However, a final model for the NNB cannot be proposed at the current stage of analysis. Several options have to be tested by modeling, which was not possible during the cruise.

Mozambique Ridge (MOZR)

The interpretations of the magnetic data gathered in 2005 across the MOZR are fully confirmed. The new lines and the resulting magnetic grid show clear magnetic stripes, which can only be interpreted as magnetic reversals. Towards the eastern and western margins, the anomalies are less pronounced. They might be overprinted/destroyed either by horizontal lava flows or younger volcanism. In the north of the MOZR magnetic grid, the anomaly pattern is terminated by a pronounced negative anomaly. At the moment, its relevance for the entire spreading system is not clear. We have to wait for the gravity data for a better interpretation of this area.

An oceanic MOZR, however, removes a lot of overlap problems in the Gondwana reconstruction models. It also shows that magmatism had a much longer geological history in the area than previously assumed. This interpretation contradicts results from analyses on dredged rock samples, which are clearly of continental origin. Thus, a model for the MOZR has to contain small terranes or basement blocks, which were embedded by basalts during the break-up. These blocks may have originated from the western side of the ridge from the Falkland Plateau, and on the eastern side from Dronning Maud Land, Antarctica. It could reflect a very long lasting and complex rift process.

8. Shipboard Three-Component Magnetometer (STCM)

Tomoko Hanyu
NIPR, Tokyo, Japan

8.1 Introduction

Magnetic anomalies at sea play an important role to elucidate seafloor-spreading history. The geomagnetic anomaly field is a vector field, and can be described by three directions, namely Northward, Eastward, and vertical components. Measuring the vector magnetic anomaly field, we can immediately quantify the strike of a boundary of magnetic anomalies, in addition to its polarity, in a single geophysical track. Consequently, the vector geomagnetic anomaly field is useful for marine geoscientists in terms of revealing seafloor tectonics, because the anomaly amplitudes from the total intensity magnetometer data are often much reduced, depending on the orientation of the ambient geomagnetic field and magnetic lineation. These orientations, however, have no effect on the three component vector anomalies.

8.2 System setup

Vector geomagnetic field data were collected by a shipboard three-component magnetometer (STCM), supplied by the National Institute of Polar Research (NIPR) in Japan, using three-axis sensors of the fluxgate (FG) type magnetometer attached on the top deck above the bridge. To obtain ship's attitude information such as yaw, roll and pitch, for example, a Ring Laser Gyro system was installed and a GPS antenna was also fixed on the top deck. The cables from the magnetometer sensors and the GPS antenna were placed to lead into the CTD room. The STCM system presented itself as shown in Figure 18 (see also A.7).

The general experimental setup of the STCM system was done as shown in figure 19. The cable of the magnetometer sensors and the GPS antenna were connected to the controller (Tierra Technica SFG-2005). The controller simultaneously sampled three-components of magnetic field in sampling intervals of 10 Hz. Those data were transmitted to the laptop computer via RS-232C and recorded. Ship's attitude information were also obtained by attitude sensors (Japan Aviation Electronics Industry, Ltd. Ring Laser Gyro, JIMS-200R) with a sampling interval of 10 Hz, and stored on a laptop.

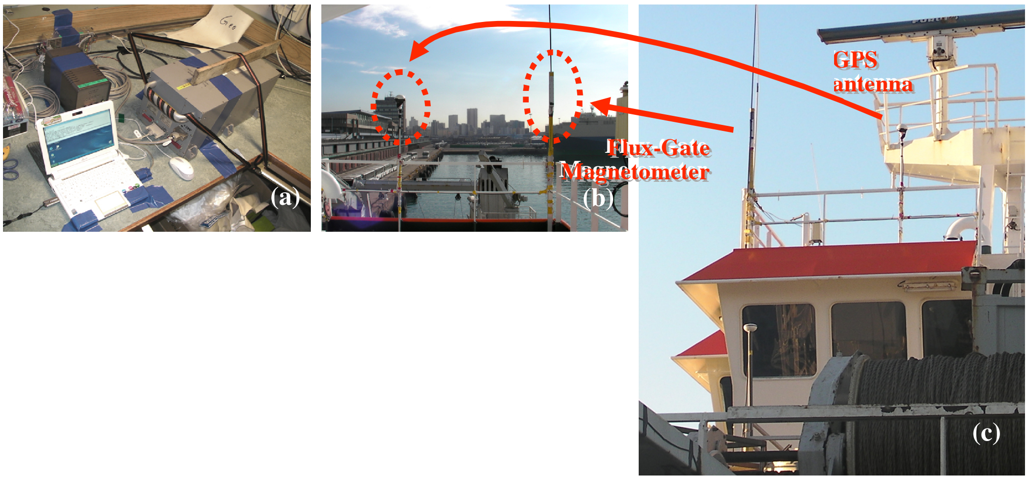

Fig. 18: Pictures of the STCM system on RV Pelagia.
(a) RLG, controller and laptop computer in the CTD room;
(b) + (c) FG sensor and GPS antenna are attached on the top deck above the bridge.

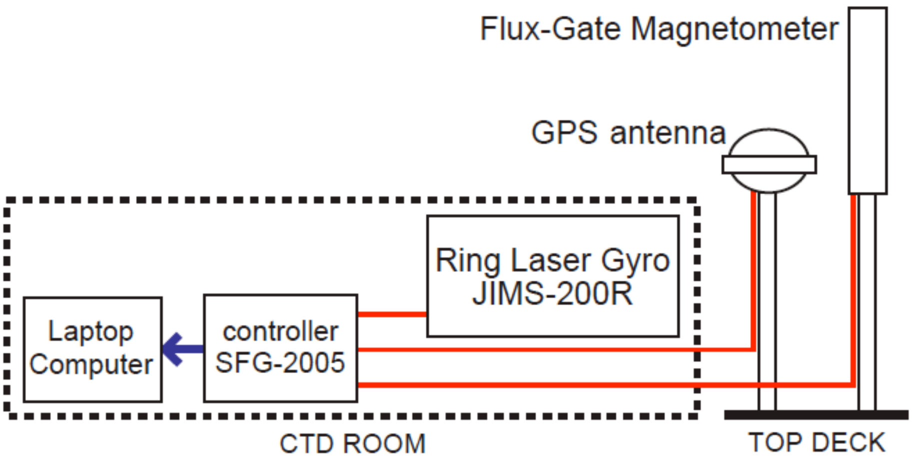

Fig. 19: Setup of the STCM system.

8.3 Calibration of the ship's magnetization

The STCM data contains the effects of the ship's magnetic field, which must be corrected in order to derive the real geomagnetic field. Twelve constants of the B and H matrix related to the ship's permanent and induced magnetic field are estimated using the data from a calibration circle called "Figure-Eight turn". The "Figure-Eight turn" is done by steering the ship in a tight circle, both in a clockwise and counter clockwise rotation, as shown in figure 20.

"Figure-Eight turns" were conducted on April 15th and 22nd, and on May 7th, 22nd, 27th, 28th and 31st of 2009, at each location shown in figure 21. To estimate the twelve constants related to the ship's magnetic field, those data will be analyzed after the cruise.

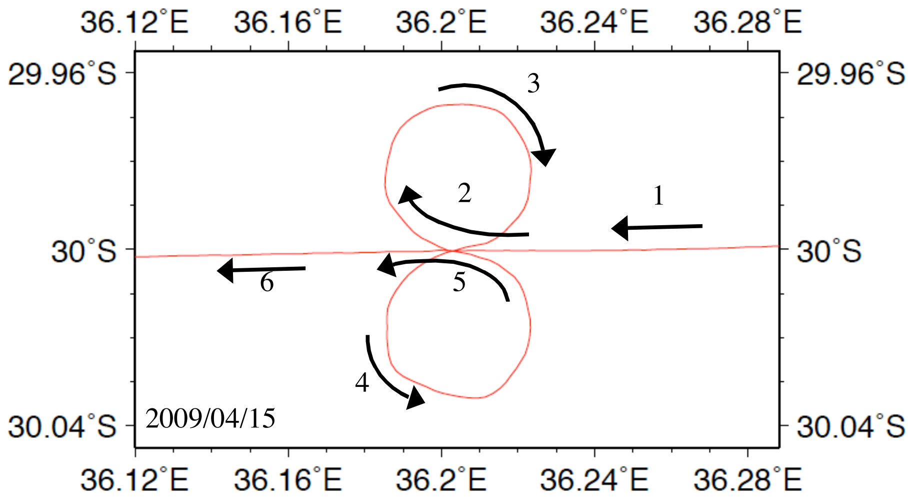

Fig. 20: Example of calibration circle trace as "figure eight turn".

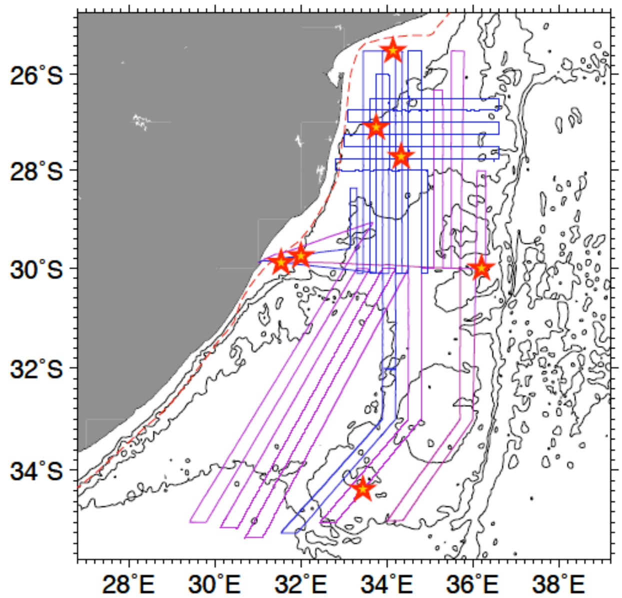

Fig. 21: Ship's sailing track during cruise RV Pelagia legs 64PE 305 & 306.

Location of Figure-Eight turns
Trace of leg 64PE305
Trace of leg 64PE306
Continental - Ocean Boundary

8.4 Observation

Vector geomagnetic field measurements with STCM were started at 05:15 UTC, on April 9th. Three-components of magnetic field and ship's attitude information (yaw, roll and pitch) were continuously acquired during the cruise.

However, a few seconds of missing data occurred every 10 seconds. This problem was perhaps due to insufficient CPU performance for graphics. After 8 days of data acquisition, the problem was fixed using simple text data mode. The other problem occurred during the last week of 1st leg, when erroneous position data appeared in the GPS data. The cause of this mistake could not be found during the cruise. The position data during this period will be corrected from RV *Pelagia*'s GPS data after the cruise. On May 29th, the power supply plug failed and the entire system was shut down at 19:10 UTC. The system was restarted at 19:21 UTC, afterward the Gyro alignment mode was started. The Gyro alignment mode was finished at 20:10 UTC, and all information were continuously obtained. For details see appendices A.8 and A.9.

Northward, eastward and vertical geomagnetic field anomalies along the ship track will be also deduced from the correction of the ship's magnetic field and the IGRF be subtracted after the cruise.

9. Echo Sounder

Mike.K. Watkeys[1)], Conrad Kopsch[2)], Volker Leinweber[2)], Michele Ickrath[2)]. *Leg 1*: Selwyn Adams[3)], Errol Wiles[1)]. *Leg 2*: Tshifhiwa Mabidi[3)], Jose Sobral[4)].

[1)]University of Kwazulu-Natal, Durban, South Africa
[2)]Alfred Wegener Institute, Bremerhaven, Germany
[3)]Petroleum Agency of South Africa, Cape Town, South Africa
[4)]University of Maputo, Maputo, Mozambique

9.1 System

The echo-sounder is a seismic system that measures the depth to the ocean floor. It may also penetrate the overlying sediments, and detect some internal structure. Such penetration is achieved with acoustic signals by using a low frequency signal. With the system used during this cruise, a 3.5 kHz 3010 MP transceiver generates a signal for emission by a transducer with a very narrow beam, and the echo returns to the transceiver. The data are recorded using Geo-Trace 8.4 software. They are saved as digital files as well as being printed as hard copies on an analogue printer (Octopus Wideline 200/138 3-channel analogue and digital recorder).

The echo-sounder system during this cruise, therefore, could be used for:

- establishing depth of the ocean floor
- recognizing different types of topography on the ocean floor
- recognizing some internal structure in the sediments on the ocean floor to depths of about 15-20 m
- identifying regions of no sedimentary cover where it might be possible to dredge the underlying basement.

All of these aspects ultimately lead to a better understanding of the origin and evolution of the topography of the ocean floor.

9.2 Controls on ocean floor topography offshore of KwaZulu-Natal and southern Mozambique

The topography of the ocean floor is dependent on three factors: the basement template, sediment input and ocean currents (Figure 22).

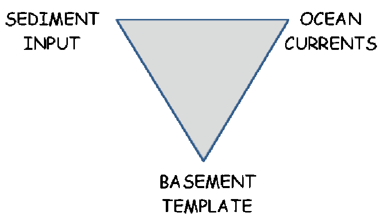

Figure 22: Three interacting factors that control ocean floor topography

The basement template

The basement template in this region may be considered in terms of five physiographic regions: continental shelf, continental slope, southern Natal Valley, northern Natal Valley and the Mozambique Ridge.

The continental shelf in extremely narrow along the N-trending KwaZulu-Natal and southern Mozambique coast but widens further north once the coast trends ENE at the southern end of the Mozambique coastal plain. Where it is narrow, it drops off rapidly down the continental slope to the abyssal plain. This slope marks the continent-ocean boundary, but here is not one involving extension normal to the coast but is a transform boundary at the northernmost extremity of the Agulhas Fracture Zone. In the southern Natal Valley, the basement is unquestionably of oceanic origin, but the nature of the basement in the northern Natal Valley is more enigmatic. This research cruise aims at resolving this problem, but the solution is outside the scope of echo-sounding. The northern Natal Valley has three ENE-tending ridges: the Tugela Ridge in the south, the Naudé Ridge slightly farther north, and the Almirante Leite Bank in the north. The Mozambique Ridge extends southwards from the SE margin of the Mozambique coastal plain, and forms the eastern boundary of the northern and southern Natal Valleys. It has been variously proposed that the basement here is either composed entirely of continental origin, or entirely of oceanic origin, or a mixture of both. This problem is yet another focus of this research cruise and, again, one that echo-sounding cannot resolve, beyond identifying exposed areas of basement as potential dredge sites.

Sediment input

The sediment in the region is primarily derived by fluvial processes that have formed the landscape of southern Africa. In the eastern parts of the subcontinent, the weathered material is largely eroded and transported by rivers to the ocean during the wet summer months.

Adjacent to the southern Natal Valley and the southern part of the northern Natal Valley, the rivers have sources in the Drakensberg, which is over 3000m high and sometimes only 200 km from the coast, and flow unimpeded down to the coast. Here, they deposit their load on the shelf and into canyons that transport it to greater depths. Not unexpectedly, the sediments are thickest adjacent to the coast. Due to the steepness of the continental slope, the shelf and upper slope sediments build up to form unstable masses that are also transported down slope as slumps and slides.

Most notable of these rivers is the Tugela with its well-developed cone offshore. However, in the past, this river was once much smaller. The upper reaches of the Tugela used to continue eastwards into the Mhlatuze River, which reaches the ocean at Richards Bay, about 100 km further north than the present Tugela mouth. The lower reaches of the Tugela eroded back up-stream, capturing the upper portions of the palaeo-Tugela/Mhlatuze, leaving a wind gap between the present courses of the Tugela and Mhlatuze.

Inland of the northern parts of the Natal Valley, the rivers are derived from lower elevations of the portion of the Great Escarpment that connects the Drakensberg to the Transvaal Escarpment. The course of these rivers to the coast is impeded by the N-S trending Lebombo range and their drainage has been superimposed on this feature. East of the Lebombo, these rivers flow across a narrow coastal plain. Here, the Mkuze River turns south into Lake St. Lucia, while the Phongola River turns north into Maputo Bay. The fish fauna in these two river systems suggests that these two drainage basins have long been separate, rather than once joining to flow. Consequently, there are no rivers currently flowing into the northern Natal Valley between Richards Bay and Maputo Bay. This lack of sediment in the water is one of the reasons for the development of coral reefs in the shallow waters of the shelf. However, this was not the case in the past when the palaeo-Phongola River once flowed across the coastal plain and into the sea at the site of Lake Sibaya, which is perched above sea-level behind the coastal dunes.

North of Maputo Bay, the rivers that flow across the Lebombo have their sources to the west of the Transvaal Escarpment. The largest of these is the Limpopo that flows northwards from the interior of South Africa, then eastwards, forming the border with Botswana and Zimbabwe, before turning to the SE and flowing over the coastal plains of Mozambique into the northern Natal Valley. It is clear that the major portion of the sediments deposited on the Mozambique Plains and the northern Natal Valley were derived from the Limpopo. In order to form the Mozambique Plains, they had to essentially fill the space that once existed between the Lebombo and the northern end of the Mozambique Ridge. These sediments have also built up the Limpopo cone, Inharrime Terrace and the extensive Central Terrace of the northern Natal Valley. However, today the river is rather small in its lower reaches and appears incapable of such a feat. In fact, it is smaller than the Save River that supplies sediments to the northern part of the Mozambique Plains. The reason for this is that the Limpopo was once a much larger river and has been reduced in size by river capture.

This river capture took place in the interior of southern Africa in NW Botswana, and involved the Shashe River. The confluence of the Limpopo and the much larger Shashe River is a triple point between South Africa, Botswana and Zimbabwe. The Shashe forms the border between Botswana and South Africa, and today its upper reaches lie in the eastern Kalahari Desert, a relatively short distance from its confluence with the Limpopo. The river's size, the short length of its present upper reaches and its source area of very low rainfall indicate that it once must have been derived from further NW across the opposite side of the Kalahari Desert. In fact, its source was in the Angolan highlands, from where it used to flow southeast across the present position of the Okavango swamps and Magadikadi pan in Botswana into the Limpopo. An uplift along ENE-trending faults in the Okavango region during the Tertiary diverted this flow. Now, in times of flood, the upper reaches of this system overflow from Okavango, into Chobe and then into the Zambezi River. Consequently, when the Limpopo River floods nowadays, its load is much reduced compared to the past and is largely deposited over the wide, flat Mozambique coastal plains as demonstrated during the major flood of 2000.

Ocean Currents

The sediment load disgorged by rivers into the ocean may be dissipated into the water column, may be deposited close to the river mouth or may travel as gravity flow along canyons cutting into across the shelf, down the slope and onto the abyssal plains. Whether in the water column or deposited as sediment, this material is subject to transport and deposition by ocean currents. In the case of this region, there are three main currents to consider. At the surface there is the Agulhas Current System, a warm current flowing southwest along the eastern seaboard of southern Africa. This current has a mean velocity of 2 m s^{-1} and extends down to a depth of 2000m. Consequently, it transports shelf and slope sediments southwards.

Inshore of the main Agulhas Current, there is a counter-current with a northerly flow. It is responsible for the development of the log spiral bays that are most obvious along the "softer" coastline of the coastal plain of northern KwaZulu-Natal and the Mozambique Plains. This inshore system is also responsible for developing the bars, which close the river mouths during the dry winter months.

Beneath this current is the northward flowing North Atlantic Deep Water, a relative newcomer that moved into the region during the early Pliocene. Underneath there is the Antarctic Bottom Water, which also flows northwards, finding its way through the deepest gaps in the Mozambique Ridge into the Mozambique Basin. This current is eroding the abyssal sediments and piling them up into the confusingly named Agulhas Drift in the Transkei Basin and the Transkei Drift in the southern Natal Valley.

9.3 First results

In the echo-sounder traces, the date, UTC time, the longitude (E) and the latitude (S: the negative number) are taken from the starting position of the survey, which is noted at the left side of the trace. The small inset diagram shows the ship's track during the survey. Vertical exaggeration varies from figure to figure.

Continental shelf
On the shelf offshore of Lake St. Lucia, north of Richards Bay, the smooth continuous surface of continental shelf is dissected by canyons up to 200 m deep than run eastwards from the coast out onto the continental slope (Fig. 23).

Southern Natal Valley:
In the southeastern parts of the southern Natal Valley, adjacent to the Mozambique Ridge, the Antarctic Bottom Current has scoured the sediments, and built up the Transkei Drift (Fig. 24). The northern end of the southern Natal Valley is marked by a transition from the smooth topography into the more rugged terrain of the South Tugela Ridge (Fig. 25).

Northern Natal Valley
In the west, the southern and northern Natal Valleys are separated by ridges and a change in elevation is obvious across the Naudé Ridge (Fig. 26). This ridge and the Tugela Ridge act as obstructions to sediment transports from N to S. They also appear to confine the Tugela cone. In the east, the northern and southern Natal valleys are separated by an ENE-trending valley, which has a marked negative magnetic anomaly. This valley also cuts into the Mozambique Ridge (Fig. 27).

A large portion of the northern Natal Valley comprises the monotonously smooth Central Terrace. At its northern end, the Almirante Leite Bank partially blocks the sediment transport from the Limpopo onto the Central Terrace and also deflects the Agulhas Current. Consequently, the Inharrime Terrace to the north is at a much higher elevation than the Central Terrace to the south (Fig. 28).

Mozambique Ridge:
On its eastern side, the Central Terrace is flanked by the rugged topography of the Mozambique Ridge (Figure 29). On the echo-sounder trace, the layering in the sedimentary cover can be seen draping over this topography (Fig. 30).

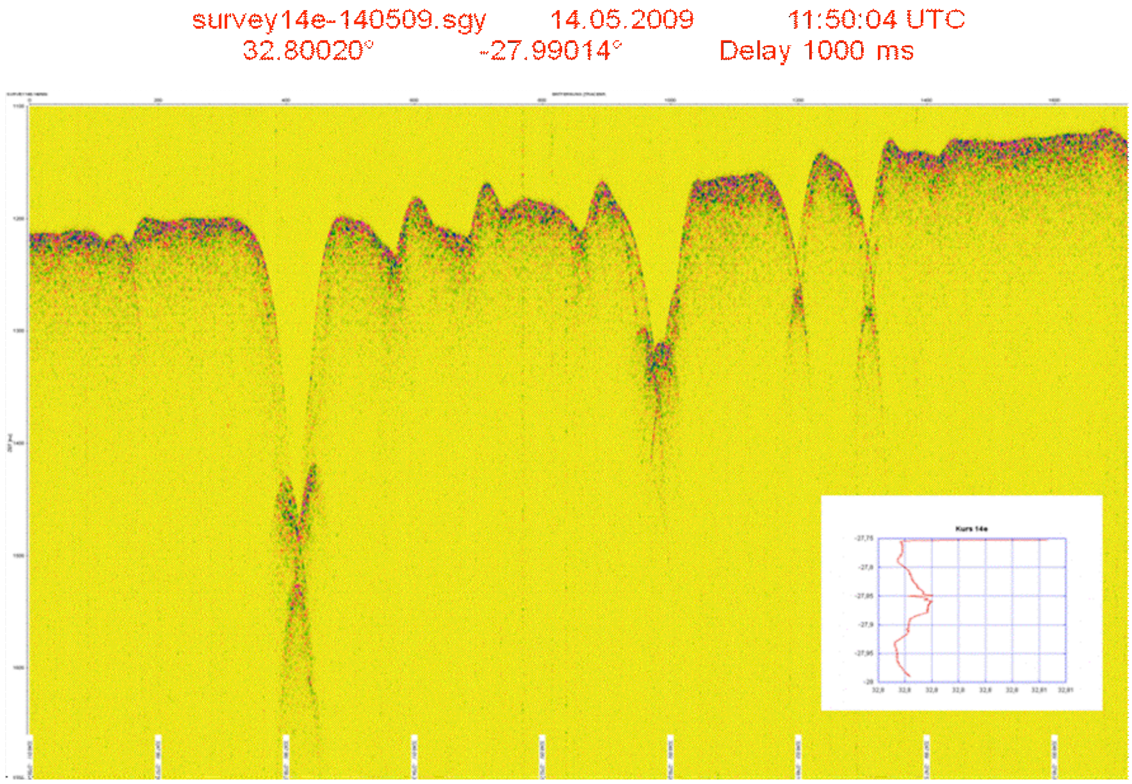

Fig. 23: S-N section, viewed looking W, of canyons offshore of Lake St Lucia. Water depths: 850-900 m

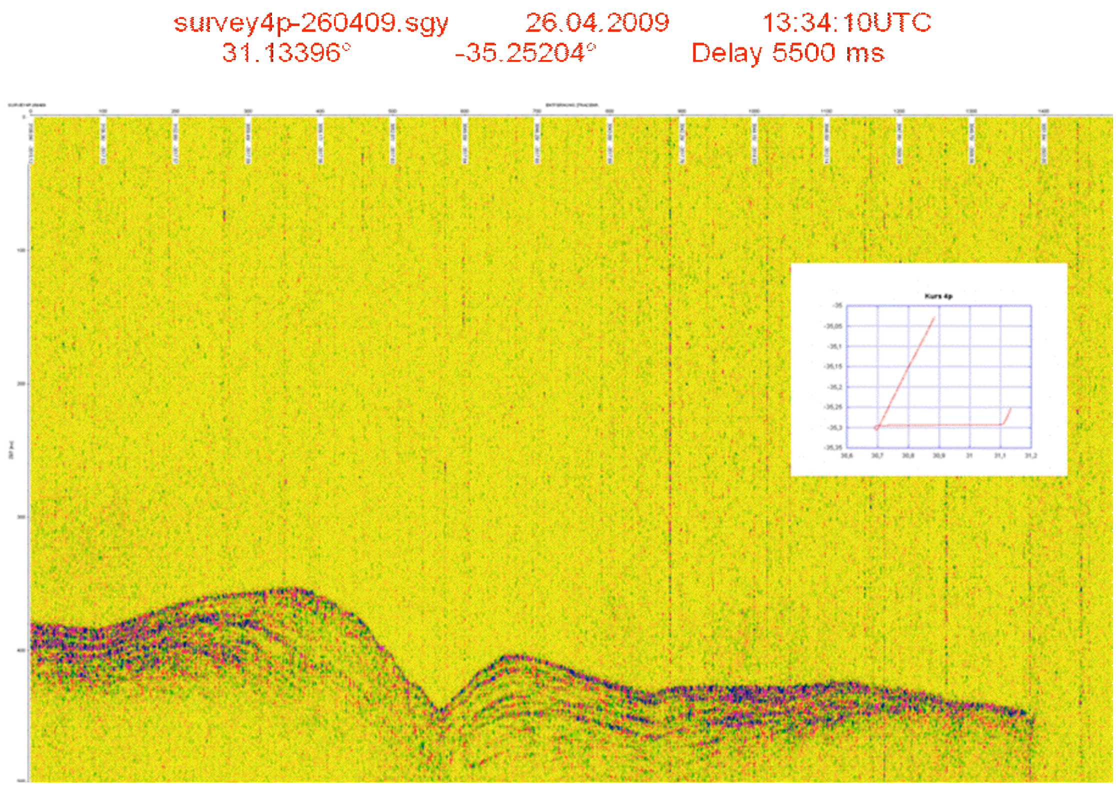

Fig. 24: E-W section, viewed towards the south of the Transkei Drift in the southern Natal Valley, just west of the south-westernmost tip of the Mozambique Ridge. Water depths: 4400 to 4500 m.

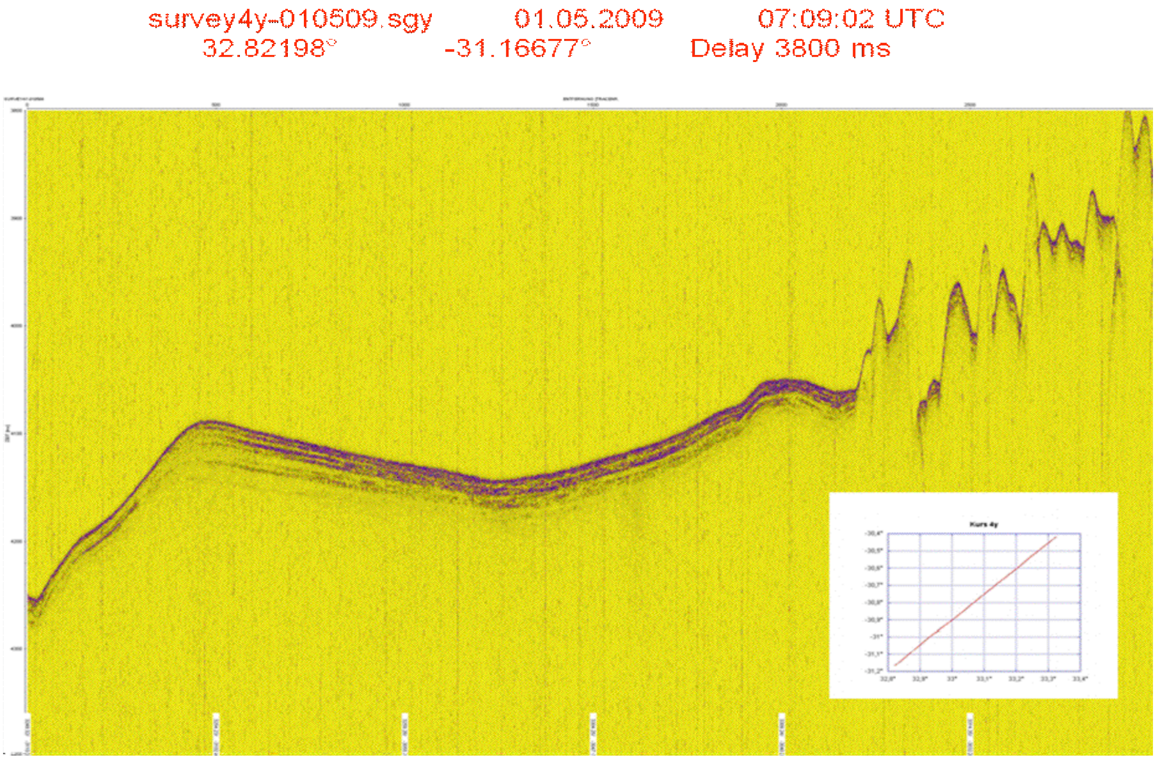

Fig. 25: S-N section, viewed towards W, of the smooth southern Natal Valley abutting against the South Tugela Ridge. Water depths: 2900-3150m.

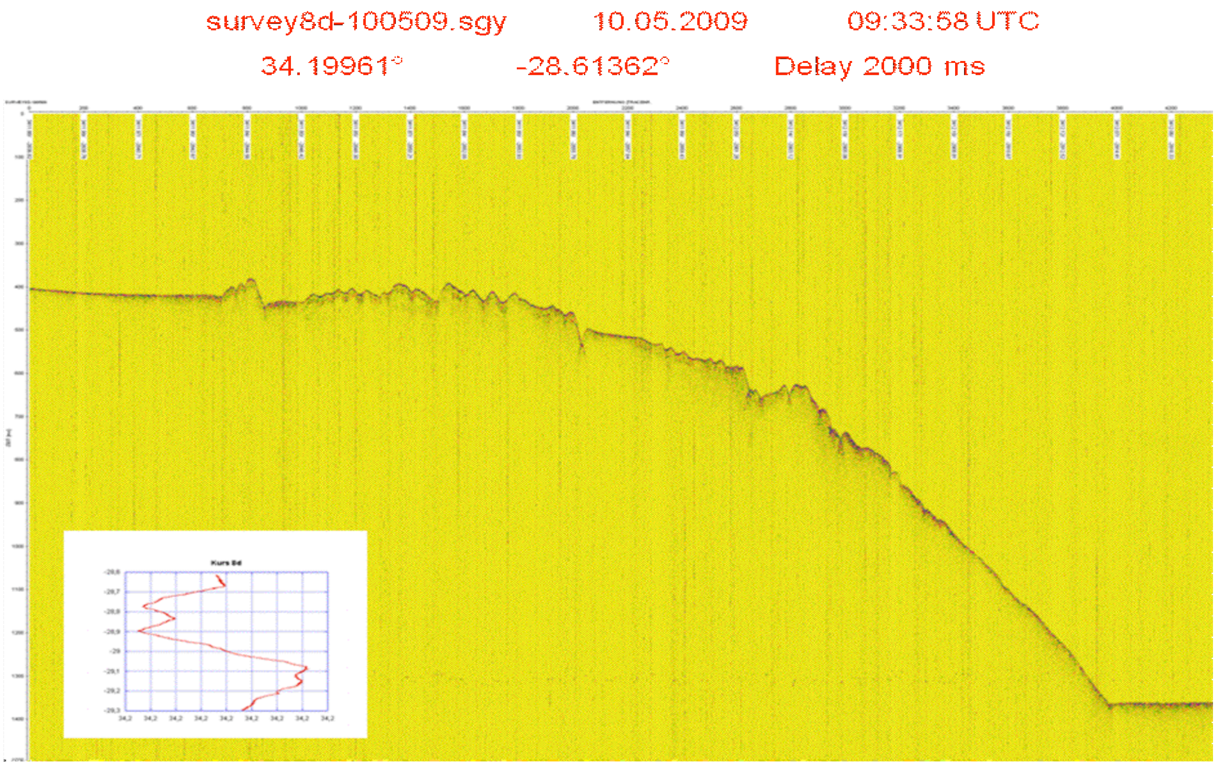

Fig. 26: N-S section, viewed towards the east of the transition from the elevated northern Natal Valley across the Naudé Ridge to the lower southern Natal Valley. Water depths: 1800-2500 m.

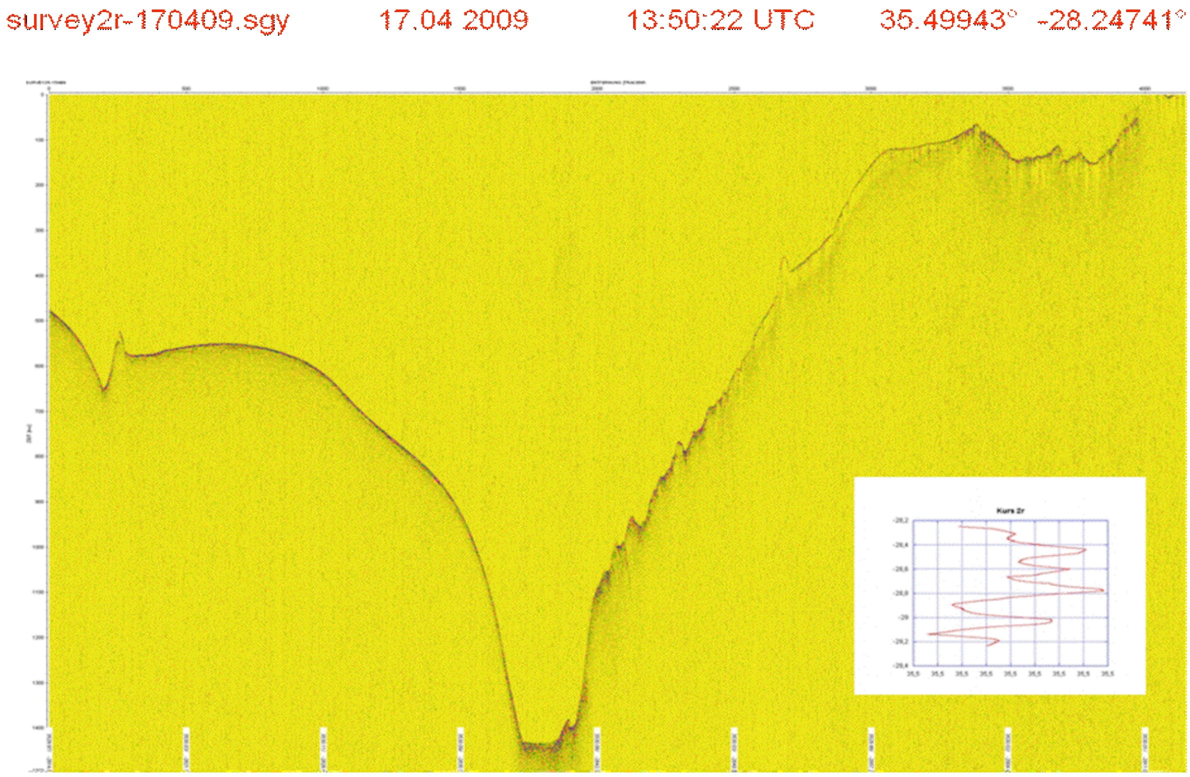

Fig. 27: W-E section viewed towards the north of an oblique section through an ENE-valley separating the smooth topography at the southern end of the northern Natal Valley from the rugged topography of the Mozambique Ridge. Water depths: 1950-2900 m

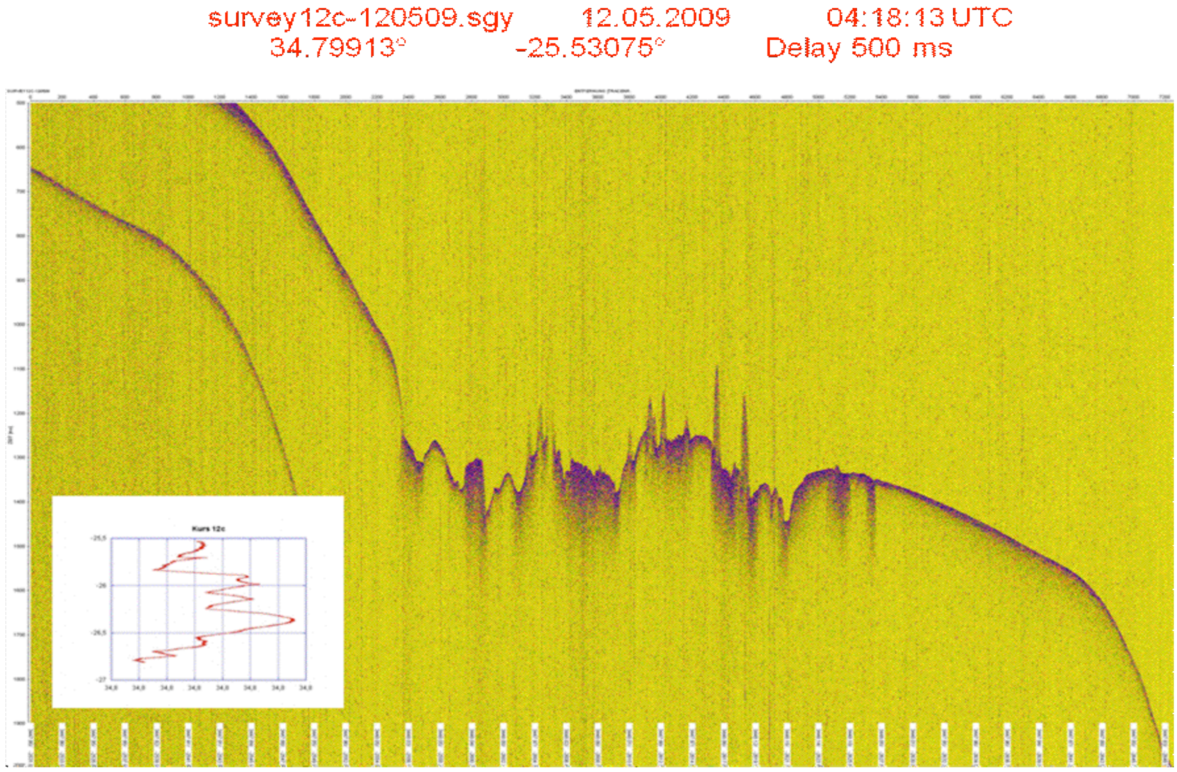

Fig. 28: N-S section, viewed towards the east of the Almirante Leite Bank with the Central Terrace to the S and the elevated Inharrime Terrace to the north, which is truncated in this figure. Water depths: 600-1500 m

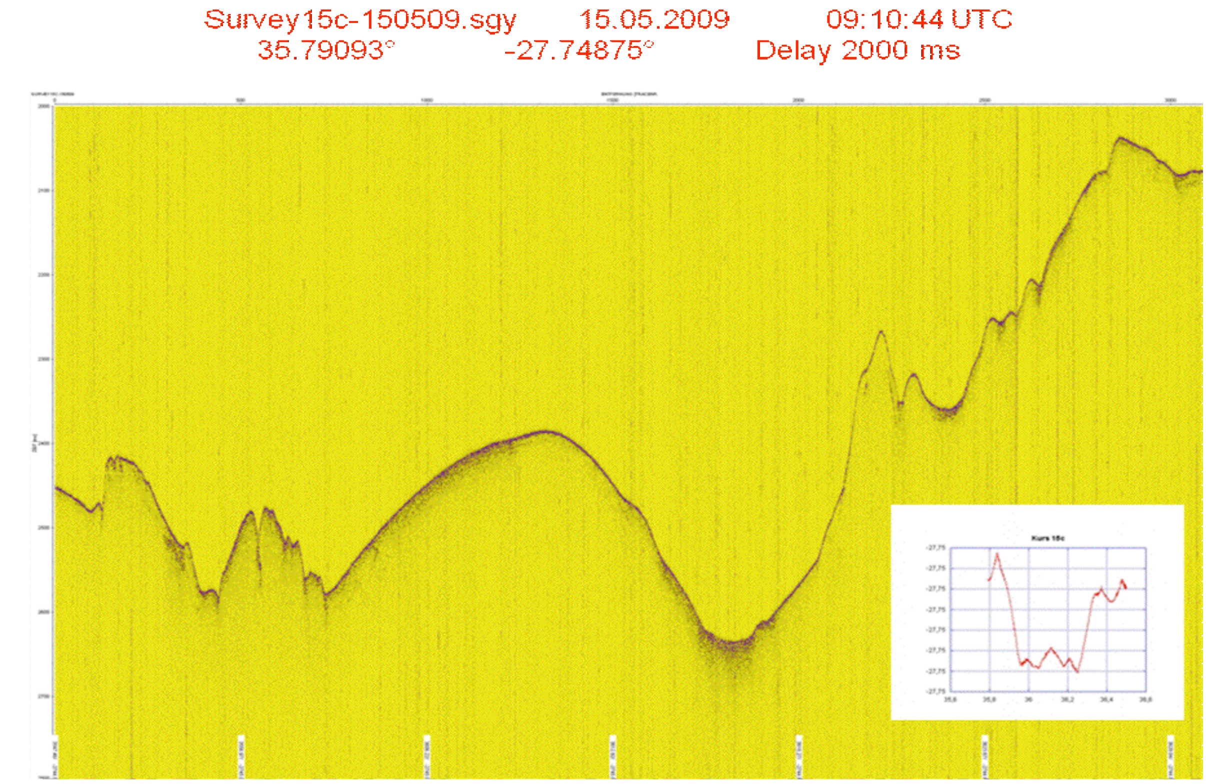

Fig. 29: W-E section, viewed towards the north from the easternmost edge of the Central Terrace of the northern Natal Valley onto the Mozambique Ridge. Water depths: 1600-2100 m

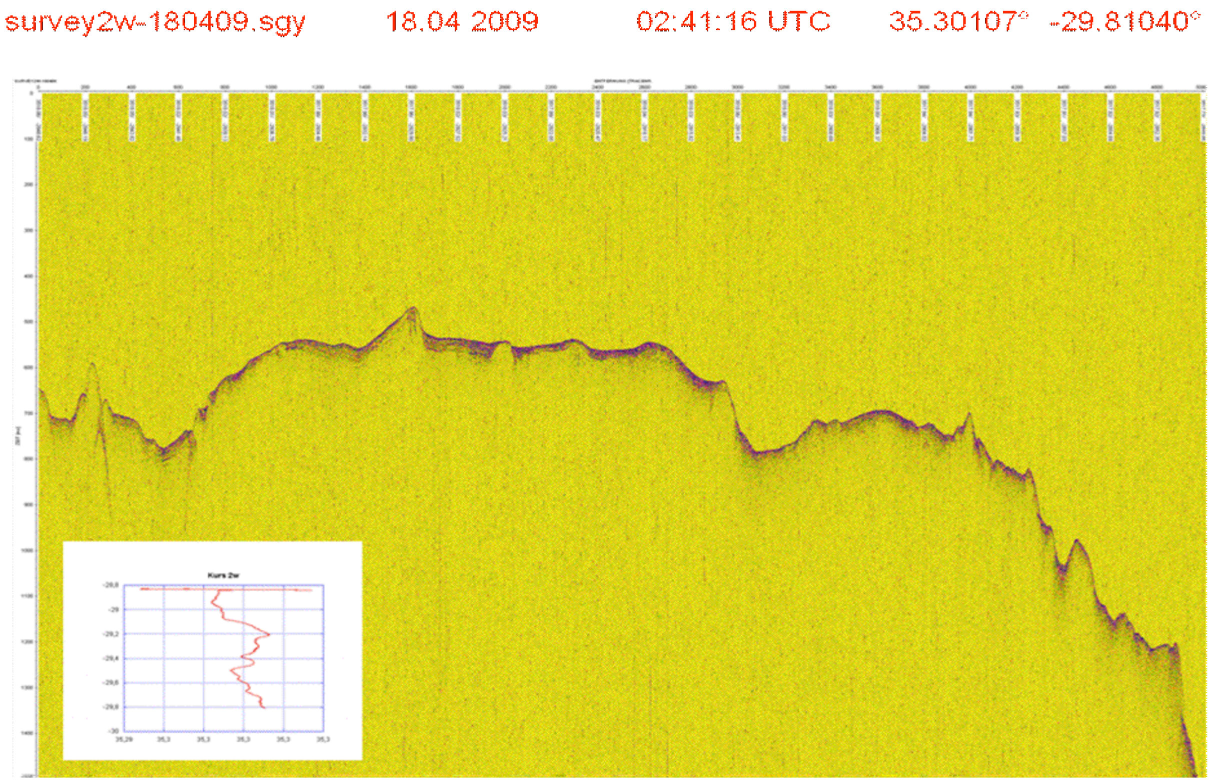

Fig. 30: S-N section, viewed towards the west of the rugged topography of the Mozambique Ridge, draped by a sedimentary cover. Water depths: 2000-2550 m.

10. Dredge Report

M.K. Watkeys[1)]
[1)]University of Kwazulu-Natal, Durban, South Africa

M. N. Ovechkina[2)] (not on board)
[2)] Joint Council for Geoscience/University of KwaZulu-Natal Marine Geoscience Unit, Durban, South Africa

10.1 Methodology

The original aim of dredging during this cruise was to collect samples of basement rocks, suspected young volcanism and manganese encrustations and nodules on the Mozambique Ridge. It was clear from previous work experience that one problem with dredging basement rocks would be both the sediment cover and the presence of a hard crust of manganese. Dredge sites were chosen by close examination of the echo-sounder profiles in conjunction with the Swath bathymetry being produced en route. Steep sections were identified as the best potential targets.

The dredge was essentially a steel pipe, 0.4m in diameter and 1.5 m long, with a grill covering the rear opening. Six teeth were welded to the leading edge in order to give it some bite. The ship was positioned at a station above the base of the chosen slope. The dredge was lowered over the stern of the ship by a winch on a steel 3-strand cable with a breaking strain of 12 tons at a rate of about 50 m/minute. Approximately 200 m of additional cable were then laid out and the ship was either allowed to drift or was sailed slowly (less than 1 knt) in the required direction for about 800 m and 1-2 nautical miles, as required. Tension on the cable was monitored to establish whether the dredge became entangled on rocks in case the strain became too high for the cable. Once the ship had drifted to the final position, the dredge was winched aboard.

During the first dredging operation at the first locality, one of the three strands on the cable broke and the dredge returned to the surface empty. An additional successful dredge was undertaken at this site. It was then decided to utilize the dredge with circumspection and to use it only on the best possible target rather than lose it while attempting to sample other less promising localities. Consequently only one other dredging operation was attempted during the cruise (Table 7).

Table 7: Summary of dredge localities

Station	Date	Dredge	Time (UTC)	Latitude	Longitude	Depth
RVP09-01a	22/04/2009	On bottom	11:33	34° 21' 59"	33° 26' 58"	1711
		Off bottom	12:33	34° 21' 43"	33 26' 26"	1682
RVP09-01b		On bottom	14:17	34° 22' 25"	33° 27' 27"	1904
		Off bottom	14:43	34° 22' 09"	33° 27' 10"	1790
RVP09-02	25/05/2009	On bottom	20:15	33° 18' 57"	33° 52' 19"	3143
		Off bottom	23:00	33° 20' 48"	33° 50' 41"	2415

10.2 Dredge site RVP09-01

This site was chosen because it was a volcanic crater which was only partially covered by a thin layer of younger material and had an elevated rim that appeared to be exposed. During the first dredging operation (RVP09-01a), the ship drifted slowly to the WNW, pulling the dredge across the ocean floor and up the rim. The dredge was hauled in before reaching the top of the rim. As mentioned above, it returned to the surface empty and with damage to the cable.

After cutting off the damaged section of the cable and reattaching it to the dredge, a second dredge took place (RVP09-01b), this time on the SE side of the crater. Here, the crater wall seemed to have partially collapsed outwards and down slope. We were hoping to sample some loose volcanic material as well as material from inside the crater. The dredging operation started at the base of the small slope and continued up NW to the edge of the collapsed rim. This time, about 0.68 m^3 of green-grey clay sediment rich in microfossils were collected. It was distributed between four boxes that were taken ashore during the mid-cruise bunkering in Durban. While the second leg was underway, the nannoplankton in the sediment was identified by Dr. M. Ovechkina. This late Pleistocene-Holocene sediment provides a minimum age of the volcanism. As the crater was only partially covered, probably by this sediment, it seems that the age of volcanism is unlikely to be much older.

Identification of calcareous nannoplankton from Dredge Site RVP09-01b
A standard method of nannoplankton identification was employed (Green *et al.*, 2008): one sample was collected from each box, with one smear slide made for each sample. All smear slides contain very representative assemblages of excellently preserved abundant nannoplankton, with 35 identified species.

Nannoplankton identified from Dredge Site RVP09-01b
The following taxa were identified in the four samples:

Algirosphaera sp.
Calcidiscus leptoporus (Murray et Blackman, 1898) Loeblich et Tappan, 1978
Calciosolenia brasiliensis (Lohmann, 1919) Young, 2003
Ceratolithus cristatus Kamptner, 1950
Ceratolithus simplex Bukry, 1979
Ceratolithus telesmus Norris, 1965
Coccolithus pelagicus (Wallich, 1877) Schiller, 1930
Discosphaera tubifera (Murray et Blackman, 1898) Ostenfeld, 1900
Emiliania huxleyi (Lohmann, 1902) Hay et Mohler, 1967
Florisphaera profunda Okada et Honjo, 1973
Gephyrocapsa ericssoni McIntyre et Be, 1967
Gephyrocapsa oceanica Kamptner, 1943
Gephyrocapsa sp.
Gephyrocapsa sp. (small)
Gladiolithus flabellatus (Halldal et Markali, 1955) Jordan et Chamberlain, 1993
Helicosphaera carteri (Wallich, 1877) Kamptner, 1954
Helicosphaera hyalina Gaarder, 1970
Helicosphaera kamptneri Hay et Mohler in Hay et al., 1967
Helicosphaera wallichii (Lohmann, 1902) Boundreaux et Hay, 1969
Oolithotus sp.
Pontosphaera discopora Schiller, 1925
Pontosphaera japonica (Takayama, 1967) Nishida, 1971

Pontosphaera multipora (Kamptner, 1948) Roth, 1970
Reticulofenestra sp.
Rhabdosphaera claviger Murray et Blackman, 1898
Rhabdosphaera sp.
Rhabdosphaera stylifer Lohmann, 1902
Syracosphaera pulchra Lohmann, 1902
Syracosphaera rotula Okada et McIntyre, 1977
Thoracosphaera heimii (Lohmann, 1919) Kamptner, 1941
Thoracosphaera saxea Stradner, 1961
Umbellosphaera irregularis Paasche in Markali & Paasche, 1955
Umbellosphaera tenuis (Kamptner, 1954) Paasche, 1955
Umbilicosphaera hulburtiana Gaarder, 1970
Umbilicosphaera sibogae (Weber-van Bosse, 1901) Gaarder, 1970

10.3 Age of the sediment from Dredge Site RVP09-01b

The zonations by Gartner (1977) and Okada & Bukry (1980) were used to establish the age of nannoplankton. They indicate that the sediment was deposited during Zone NN21 or CN15 (Upper Pleistocene–Holocene). This is based on the presence of *Emiliania huxleyi*, the first occurrence of which delineates the lower boundary of this zone.

Dredge site RVP09-02

This dredge site is situated on the SW flank of the Du Toit Graben. It is SE of a previous dredging operation which produced meta-pelitic rocks, akin to those found onshore in KwaZulu-Natal in the ca. 1000 Ma Namaqua-Natal Metamorphic Province (Ralliard, 1990). Despite dredging up a steep slope, no rocks were collected. Due to impending weather conditions, a second dredging operation was not attempted at this locality.

References

Green A, Ovechkina MN, Uken R (2008). Nannofossil age constraints for the northern KwaZulu-Natal shelf edge wedge: Implications for continental margin dynamics, South Africa, SW Indian Ocean. Continental Shelf Research 28, 2442–2449.

Gartner S (1977). Calcareous nannofossil biostratigraphy and revised zonation of the Pleistocene. Marine Micropaleontology 2, 1–25.

Okada H, Bukry D (1980). Supplementary modification and introduction of code numbers to the low-latitude coccolith biostratigraphic zonation (Bukry, 1973; 1975). Marine Micropaleontology 5, 321–325.

Appendix

A.1 TEILNEHMENDE INSTITUTE / PARTICIPATING INSTITUTIONS

	Adresse / Address
AWI	Stiftung Alfred-Wegener-Institut für Polar- und Meeresforschung in der Helmholtz-Gemeinschaft Postfach 120161 27515 Bremerhaven Germany
DURB	School of Geological Sciences Westville Campus University of KwaZulu-Natal Durban 4001 South Africa
EMU	Eduardo Mondlane University Department of Geology Maputo, PO Box 257 Mozambique
NIOZ	Royal Netherlands Institute for Sea Research Landsdiep 4 1797 SZ ‘t Horntje (Texel) The Netherlands
NIPR	National Institute of Polar Reseach 1-9-10 Kaga, Itabashi, Tokyo, 173-8515, Japan
PASA	Petroleum Agency of South Africa 151 Frans Conradie Drive Parow, 7500, South Africa
JSC	Joint Council for Geoscience/University of KwaZulu-Natal Marine Geoscience Unit, Durban

A.2 FAHRTTEILNEHMER / CRUISE PARTICIPANTS

1st Leg

Name	First Name	Nationality	Institution
Adams	Selwyn	South African	PARSA
Damaske	Daniel	German	AWI
Groenewegen	Ruud	Netherlands	NIOZ
Hanyu	Tomoko	Japanese	NIPR
Ickrath	Michèle	German	AWI
Jokat	Wilfried	German	AWI
Kopsch	Conrad	German	AWI, Potsdam
Krocker	Ralf	German	AWI
Leinweber	Volker Thor	German	AWI
Reinshagen	Sarah	German	AWI
Watkeys	Michael	British	Durban University
Wiles	Erol	South African	Durban University

2nd Leg

Name	First Name	Nationality	Institution
Cludray	John	British	NIOZ
Damaske	Daniel	German	AWI
Hanyu	Tomoko	Japanese	NIPR
Ickrath	Michèle	German	AWI
Jokat	Wilfried	German	AWI
Kopsch	Conrad	German	AWI, Potsdam
Krocker	Ralf	German	AWI
Leinweber	Volker Thor	German	AWI
Mabidi	Tshifhiwa	South African	PARSA
Reinshagen	Sarah	German	AWI
Sobral	Jose	Mosambique	University Maputo
Watkeys	Michael	British	Durban University

A.3 SCHIFFSBESATZUNG / SHIP'S CREW

1st Leg

No.	Last Name	First Name	Rank
1	Ellen	John	Master
2	van Haaren	Joep	Chief Officer
3	Verheyen	David	2nd Officer
4	Seepma	Jaap	Chief Engineer
5	Frankfort	Marco	2nd Engineer
6	Mik	Garl	Cook
7	Aleksejevs	Vitali	Steward
8	van der Heide	Roel	Ship's Technician
9	Maas	Sjaak	Ship's Technician
10	Vermeulen	Ger	Ship's Technician
11	Vitoria	Jose	Ship's Technician

2nd Leg

No.	Last Name	First Name	Rank
1	Ellen	John	Master
2	van Haaren	Joep	Chief Officer
3	Everduin	Cynthia	2nd Officer
4	Seepma	Jaap	Chief Engineer
5	de Kleine	Marcel	2nd Engineer
6	Mik	Garl	Cook
7	Aleksejevs	Vitali	Steward
8	van der Heide	Roel	Ship's Technician
9	Maas	Sjaak	Ship's Technician
10	Vermeulen	Ger	Ship's Technician
11	Vitoria	Jose	Ship's Technician

A.4 STATIONSLISTE / STATION LIST AISTEK III

Date	Time	Latitude	Longitude	Distanc e	Wdepth	Speed	Instrument
09-Apr-2009	18:00:00	29° 52' S	31° 4' E	NaN	4	9	DURBAN
10-Apr-2009	15:15:15	29° 55' S	34° 4' E	156,2	2669	9	waypoint
11-Apr-2009	00:42:38	30° 0' S	35° 42' E	85,1	2007	8,5	waypoint
11-Apr-2009	06:50:15	31° 5' S	35° 42' E	65	2495	9	waypoint
11-Apr-2009	19:12:15	33° 0' S	35° 42' E	115,1	1567	8,5	waypoint
12-Apr-2009	14:30:15	34° 48.06' S	34° 9.12' E	132,8	2560	8,5	waypoint
12-Apr-2009	16:57:15	35° 0' S	34° 0' E	14,1	2953	8,5	waypoint
12-Apr-2009	18:52:15	34° 57' S	34° 22.2' E	18,4	2501	8,5	waypoint
13-Apr-2009	11:37:48	33° 0' S	36° 0' E	142,5	1914	8,5	waypoint
13-Apr-2009	13:30:15	32° 33.94' S	36° 0.28' E	26,1	1986	8,5	waypoint
13-Apr-2009	22:15:15	31° 13.88' S	36° 1.8' E	80,1	3014	8,5	waypoint
14-Apr-2009	09:35:15	29° 24.12' S	36° 4.26' E	109,9	1956	8,5	waypoint
14-Apr-2009	18:36:15	28° 0' S	36° 6' E	84,2	1933	8,5	waypoint
14-Apr-2009	19:51:06	28° 0' S	36° 18' E	10,6	1961	8,5	waypoint
15-Apr-2009	08:37:01	30° 0' S	36° 18' E	120,1	2001	8,5	waypoint
15-Apr-2009	13:08:00	30° 0' S	35° 42' E	31,2	2007	8,5	waypoint
16-Apr-2009	08:49:59	26° 57.48' S	35° 46.08' E	182,7	1762	8,5	waypoint
16-Apr-2009	18:37:00	25° 30' S	35° 48' E	87,6	1637	8,5	waypoint
16-Apr-2009	20:07:00	25° 30' S	35° 30' E	16,3	1160	8,5	waypoint
17-Apr-2009	14:05:00	28° 17.16' S	35° 30' E	167,3	2406	8,5	waypoint
18-Apr-2009	00:09:59	30° 0' S	35° 30' E	102,9	2054	8,5	waypoint
18-Apr-2009	01:23:24	30° 0' S	35° 18' E	10,4	2188	8,5	waypoint
18-Apr-2009	08:50:00	28° 56.76' S	35° 17.88' E	63,3	2188	8,5	waypoint
18-Apr-2009	15:55:00	27° 54.7' S	35° 17.88' E	62,1	1885	8,5	waypoint
19-Apr-2009	03:03:54	26° 20' S	35° 18' E	94,8	1201	8,5	waypoint
19-Apr-2009	04:19:52	26° 20' S	35° 6' E	10,8	1006	8,5	waypoint
19-Apr-2009	08:36:59	27° 12.72' S	35° 6' E	52,8	1561	8,5	waypoint
20-Apr-2009	04:18:35	30° 0' S	35° 6' E	167,4	2404	8,5	waypoint
20-Apr-2009	06:08:42	30° 0' S	34° 48' E	15,6	2571	8,5	waypoint
20-Apr-2009	12:31:01	31° 18' S	34° 48' E	78,1	2784	8,5	waypoint
20-Apr-2009	17:42:00	31° 42.06' S	34° 48' E	24,1	2691	8,5	waypoint
21-Apr-2009	08:13:00	32° 39' S	34° 47.88' E	57	1490	8,5	waypoint
21-Apr-2009	12:00:00	33° 0' S	34° 48' E	21	1490	8,5	waypoint
21-Apr-2009	15:38:00	33° 15' S	34° 33.22' E	19,5	1465	8,5	waypoint
22-Apr-2009	11:00:00	34° 21.9' S	33° 27' E	86,7	2140	8,5	DRG
22-Apr-2009	17:15:00	34° 34.8' S	33° 13.8' E	16,9	2337	8,5	CTD/RO
22-Apr-2009	22:46:09	35° 0' S	32° 48.6' E	32,6	2879	8,5	waypoint
23-Apr-2009	00:52:52	35° 0' S	32° 26.7' E	18	3529	8,5	waypoint
23-Apr-2009	08:22:00	34° 13.74' S	33° 14.34' E	60,7	1645	8,5	waypoint
23-Apr-2009	13:33:00	33° 40.8' S	33° 48.3' E	43,4	2513	8,5	waypoint
23-Apr-2009	19:55:00	33° 0' S	34° 30' E	53,7	1619	8,5	waypoint
24-Apr-2009	10:05:00	31° 18.6' S	34° 30' E	101,5	2912	8,5	waypoint
24-Apr-2009	15:20:00	30° 44.82' S	34° 30.12' E	33,8	2754	8,5	waypoint
25-Apr-2009	00:45:00	30° 0' S	34° 30' E	44,9	2638	8,5	waypoint
25-Apr-2009	07:40:00	31° 10.8' S	33° 45.42' E	80,6	3118	8,5	waypoint
25-Apr-2009	13:24:00	31° 54.12' S	33° 18' E	49,3	3489	8,5	waypoint
26-Apr-2009	08:18:00	34° 30.12' S	31° 37.38' E	177,4	4038	8,5	waypoint
26-Apr-2009	14:00:00	35° 17.68' S	31° 6.47' E	53,9	4217	8,5	waypoint

Date	Time	Latitude	Longitude	Distance	Wdepth	Speed	Instrument
26-Apr-2009	16:30:00	35° 17.68' S	30° 42.34' E	19,7	4378	8,5	waypoint
27-Apr-2009	08:00:00	33° 13.56' S	32° 5.82' E	142,1	3749	8,5	waypoint
28-Apr-2009	06:50:00	30° 0' S	34° 12' E	221,5	2681	8,5	waypoint
28-Apr-2009	09:00:00	30° 0' S	33° 54' E	15,6	2692	8,5	waypoint
28-Apr-2009	13:15:00	30° 35.4' S	33° 30.6' E	40,8	2944	8,5	waypoint
29-Apr-2009	08:35:00	33° 24.72' S	31° 40.14' E	193,6	3851	8,5	waypoint
29-Apr-2009	22:20:00	35° 6.54' S	30° 31.2' E	116,8	4319	8,5	waypoint
29-Apr-2009	22:30:00	35° 6.36' S	30° 7.7' E	19,2	4412	8,5	waypoint
30-Apr-2009	08:08:00	33° 54.9' S	30° 57.54' E	82,5	3992	8,5	waypoint
01-May-2009	08:31:00	30° 59.39' S	32° 56.22' E	202,2	3162	8,5	waypoint
01-May-2009	16:15:00	30° 0' S	33° 36' E	68,6	2656	8,5	waypoint
01-May-2009	18:00:00	30° 0' S	33° 18' E	15,6	2527	8,5	waypoint
02-May-2009	12:00:00	32° 21' S	31° 40.8' E	163,8	3597	8,5	waypoint
03-May-2009	09:20:00	35° 0' S	29° 48' E	184,8	4337	8,5	waypoint
03-May-2009	11:20:00	35° 0' S	29° 24' E	19,7	4315	8,5	waypoint
04-May-2009	07:15:00	32° 32.7' S	31° 11.52' E	172,4	3608	8,5	waypoint
05-May-2009	11:00:00	29° 4.9' S	33° 40' E	244	2301	8,5	waypoint
06-May-2009	05:00:00	29° 52' S	31° 4' E	143,8	4	8,5	Durban-Einlaufen
07-May-2009	09:00:00	29° 52' S	31° 4' E	0,0E+01	4	8,5	DURBAN
07-May-2009	12:15:00	29° 53' S	31° 33.5' E	25,6	489	8,5	CC-Magnetik
08-May-2009	04:39:27	30° 6' S	33° 54' E	122,5	2721	8,5	waypoint
08-May-2009	08:20:00	29° 19.2' S	33° 53.4' E	46,8	2487	8,5	waypoint
08-May-2009	14:55:00	28° 20.4' S	33° 54' E	58,8	1794	8,5	waypoint
09-May-2009	08:30:00	25° 30' S	33° 54' E	170,5	334	8,5	waypoint
09-May-2009	10:15:00	25° 30' S	34° 12' E	16,3	353	8,5	waypoint
10-May-2009	07:30:00	28° 18.6' S	34° 11.4' E	168,7	1809	8,5	waypoint
10-May-2009	19:20:00	30° 6' S	34° 12' E	107,5	2703	8,5	waypoint
10-May-2009	21:50:00	30° 6' S	34° 30' E	15,6	2651	8,5	waypoint
11-May-2009	07:30:00	28° 33.6' S	34° 29.4' E	92,5	1967	8,5	waypoint
12-May-2009	02:15:00	25° 30' S	34° 30' E	183,7	333	8,5	waypoint
12-May-2009	04:15:01	25° 30' S	34° 48' E	16,3	274	8,5	waypoint
12-May-2009	21:30:00	28° 23.79' S	34° 48' E	173,9	1971	8,5	waypoint
13-May-2009	07:50:00	30° 6' S	34° 48' E	102,3	2569	8,5	waypoint
13-May-2009	08:50:00	30° 6' S	34° 57' E	7,8	2519	8,5	waypoint
13-May-2009	23:40:00	28° 0' S	34° 57' E	126,1	1903	8,5	waypoint
14-May-2009	11:45:00	28° 0' S	32° 48' E	114	826	8,5	waypoint
14-May-2009	13:45:00	27° 45' S	32° 48' E	15	603	8,5	waypoint
15-May-2009	07:40:00	27° 45' S	35° 33.6' E	146,7	1826	8,5	waypoint
15-May-2009	13:32:34	27° 45' S	36° 30' E	49,9	1925	8,5	waypoint
15-May-2009	14:10:04	27° 45' S	36° 36' E	5,3	1940	8,5	waypoint
15-May-2009	16:55:00	27° 30' S	36° 36' E	15	1930	8,5	waypoint
16-May-2009	11:55:00	27° 30' S	33° 0' E	191,7	1135	8,5	waypoint
16-May-2009	14:15:00	27° 15' S	33° 0' E	15	900	8,5	waypoint
17-May-2009	12:20:00	27° 15' S	36° 36' E	192,2	1930	8,5	waypoint
17-May-2009	15:30:00	27° 0' S	36° 36' E	15	1981	8,5	waypoint
18-May-2009	12:05:00	27° 0' S	33° 6' E	187,2	737	8,5	waypoint
18-May-2009	14:00:01	26° 45' S	33° 6' E	15	404	8,5	waypoint
19-May-2009	10:30:00	26° 45' S	36° 36' E	187,7	1996	8,5	waypoint
19-May-2009	12:00:00	26° 30' S	36° 36' E	15	1999	8,5	waypoint
20-May-2009	03:45:00	26° 30' S	33° 36' E	161,2	715	8,5	waypoint
20-May-2009	14:50:00	28° 5.76' S	33° 36' E	95,8	1652	8,5	waypoint

Date	Time	Latitude	Longitude	Distance	Wdepth	Speed	Instrument
21-May-2009	04:00:00	30° 6' S	33° 36' E	120,3	2688	8,5	waypoint
21-May-2009	05:00:00	30° 6' S	33° 45' E	7,8	2713	8,5	waypoint
21-May-2009	07:50:00	29° 41.4' S	33° 44.4' E	24,6	2602	8,5	waypoint
22-May-2009	02:07:41	27° 6' S	33° 45' E	155,5	1097	8,5	CC-Magnetik
22-May-2009	10:30:00	26° 0' S	33° 45' E	66	528	8,5	waypoint
22-May-2009	12:20:00	26° 0' S	34° 3' E	16,2	585	8,5	waypoint
22-May-2009	18:40:00	27° 2.4' S	34° 3' E	62,4	1141	8,5	waypoint
23-May-2009	12:05:00	30° 6' S	34° 3' E	183,7	2717	8,5	waypoint
23-May-2009	13:00:00	30° 6' S	33° 54' E	7,8	2721	8,5	waypoint
24-May-2009	06:15:00	33° 0' S	33° 54' E	174,1	2436	8,5	waypoint
24-May-2009	08:00:01	33° 12.6' S	33° 39.6' E	17,5	2432	8,5	waypoint
25-May-2009	00:45:01	35° 12' S	31° 21' E	165,6	4149	8,5	waypoint
25-May-2009	02:55:00	35° 12' S	31° 48' E	22,1	4034	8,5	waypoint
25-May-2009	19:00:00	33° 19' S	33° 52' E	152,7	2479	8,5	DRG
26-May-2009	03:28:53	33° 0' S	34° 12' E	25,3	1985	8,5	waypoint
26-May-2009	10:30:00	32° 0' S	34° 12' E	60	3030	8,5	waypoint
26-May-2009	12:40:00	32° 0' S	33° 54' E	15,3	3240	8,5	waypoint
26-May-2009	14:27:50	32° 0' S	34° 12' E	15,3	3030	8,5	waypoint
27-May-2009	03:53:05	30° 6' S	34° 12' E	114,1	2703	8,5	waypoint
27-May-2009	04:48:05	30° 6' S	34° 21' E	7,8	2681	8,5	waypoint
27-May-2009	07:50:00	29° 13.8' S	34° 21' E	52,2	2475	9,5	waypoint
27-May-2009	18:00:00	27° 42' S	34° 21' E	91,9	1562	9,5	CTD/RO
28-May-2009	10:54:59	25° 30' S	34° 21' E	132,1	349	9,5	waypoint
28-May-2009	12:10:00	25° 30' S	34° 7' E	12,6	350	9,5	CC-Magnetik
28-May-2009	16:40:00	25° 30' S	33° 27' E	36,1	213	9,5	waypoint
29-May-2009	07:00:00	27° 52.8' S	33° 27' E	142,9	1517	9,5	waypoint
29-May-2009	19:50:00	30° 6' S	33° 27' E	133,3	2638	9,5	waypoint
29-May-2009	20:52:00	30° 6' S	33° 18' E	7,8	2540	9,5	waypoint
30-May-2009	05:20:00	29° 12' S	33° 18' E	54	2192	8,5	waypoint
30-May-2009	11:00:00	28° 21.6' S	33° 18' E	50,4	1753	8,5	waypoint
30-May-2009	11:50:00	28° 21.6' S	33° 9' E	7,9	1675	8,5	waypoint
30-May-2009	15:30:00	28° 52.8' S	33° 9' E	31,2	1979	8,5	waypoint
30-May-2009	20:35:09	29° 36' S	33° 9' E	43,2	2201	8,5	waypoint
31-May-2009	00:54:58	29° 40.5' S	32° 27' E	36,8	1519	8,5	waypoint
31-May-2009	03:43:37	29° 45' S	32° 0' E	23,9	1023	8,5	CC-Magnetik
31-May-2009	11:46:46	29° 52' S	31° 4' E	49,1	4	8,5	DURBAN

A.5 Gravity Units

The unit of gravitational measurement is Gal named after Galileo and is 1 cm/s^2.

This unit is too large for geophysical prospecting so one uses either Milligals $[mGal]$ or Microgals $[\mu Gal]$. Occasionally one may come across the gravity unit $[gu]$.

The relationships are:
1 Gal = 1 cm/s^2 the earth field is approximately 981 Gal,
1 $mGal$ = 0.001 Gal,
1 μGal = 0.000001 Gal = 0.001 $mGal$,
1 gu = 0.0001 Gal

The unit most used in marine gravity surveys is $mGal$:
1 $mGal$ l = 10 gu = 1000 μGal = 0.001 Gal

The earth's gravity field varies from 978 Gal at the equator (0° latitutde) to 983 Gal at the poles (90° latitude).

A.6 Checklist for installation and testing the L&R S56 air/sea gravity meter system

INSTALLATION OF SENSOR IN FRAME

- Remove lid of gravity box cage
- Before moving the sensor box:
  Ensure that the sensor is clamped
- Cable connections
  - 230 VAC power on host computer (laptop)
  - 230 VAC power on UPS (check if loaded)
  - host computer – board computer (serial)
  - host computer – grav. Platform control box (serial)
  - pulse stretcher – board computer (or GPS PPS)
  - (if GPS PPS is not available use manual switch)
- Check if gimbal leveling screws are secured
- Balance sensor in gimbal frame
- Fix 3 screws in bottom of sensor box
- Connect cable to sensor
- (Check shockmount airpressure, airborne)

POWER ON SENSOR

Switch on UPS
Press two breakers on ZLS power supply unit
Check if heater lamps are burning
Check main power in host computer
Start host computer program:
switch on host computer
choose “no cardworks”
type “ultra”
ULTRASYS will start
Symbols for heat up procedure on screen?
Check pressure gauge value [expected values: 27.4 to 28.5]
Wait for:
thermostating
spin up of gyros
answer question: to unclamp the beam with: N
program starts displaying numerical values
Equalize on/off intervalls of meter heater (lowest) lamp (pot)
Check ST is off (Ultrasys: S, [3,] –9)
Check alarm off (Ultrasys: S, [4,] –9)
Check sync of ST on S56 with PC value
If out of sync set ST to counter value (Ultrasys: P, 4, xx, -9)
Replace MYLINE by new line name, (Ultrasys: P, 1, xx, –9)
Check serial output
1 or 10 sec, long format (Ultrasys: C, 2, -8, -9, -9) 10
HighRes (Ultrasys: P, -9)

GRAVITY: PRE-SENSOR CHECKS

LEVELLING PLATFORM

- Check platform levelling
- Adjust if required

BEAM CHECK

Check ST off (Ultrasys: S, [3,] –9)
Check beam zero
clamp beam twice
if abs(raw beam) > 10 adjust zero screw
until abs(raw beam) < 10
Check beam gain
unclamp beam
press CRTL-U on host computer to slew beam up
if raw beam .ne. 9000 +/- 20 adjust gain screw
press CRTL-U on host computer to stop slewing
check beam position
press CRTL-D on host computer to slew beam to 0
press CRTL-D on host computer to stop slewing
Check beam zero once more and adjust again if necessary
Slew ST abs to base reading xx if available (Ultrasys: P, 8, 1, xx, -9)

BASE READING

Check platform levelling
adjust if required
Unclamp beam (wait until TC moves down)
Check synch of ST
Turn ST on (Ultrasys: S, 3, -9)
Wait until TC < 1.0, abs(raw beam) < 2, DG ≈ base reading ST
Carry out 5 readings every 30 seconds, (note in log pages)

K-CHECK

ST: 9349,0 TC: -0,1
Turn ST off (Utrasys: S, 3, -9)
Slew ST relative by +30 (Ultrasys: P, 8, 2, 30, -9)
Wait until TC is stable (~ 15 min)
ST: 9379,0 TC: -30,0
Slew ST relative by -60 (Ultrasys: P, 8, 2,-60, -9)
Wait until TC is stable (~ 15 min)
ST: 9319,0 TC: 30.0
Slew ST relative by +30 (Ultrasys: P, 8, 2, 30, -9)
Wait until TC is stable (~ 15 min)

If TC values are within 5% of the slewed values, then k-factor ok

- Check ST off (Ultrasys: S, [3,] –9)
- Clamp beam
- Set alarm on (Ultrasys: S, 4, -9)

GENERAL CHECKS

Check for platform tilts
Check synch of ST

BASE READING (after survey)

- Check air temperature
- Check temperature of ZLS control unit
- Check platform levelling
    - Adjust if required
- Unclamp beam (wait until TC moves down)
- Check synch of ST
- Turn ST on (Ultrasys: S, 3, -9)
- Wait until TC < 1.0, abs (raw beam) < 2, DG ≈ base reading ST
- Carry out 5 readings every 30 seconds, (note in log pages)
- Turn ST off (Ultrasys: S, [3,] –9)
- Clamp Beam
- Set torque motors off (Ultrasys: S, 2,-9)
- Secure Plattform of gravitymeter with PU-Dampers

GRAVITY AFTER SURVEY PROCEDURES

- Slew ST to parking position
- Switch off gravity system (Ultrasys: P, 9, y)
    - Switch off host computer
    - Press two breakers on ZLS power supply unit
    - Switch off UPS
- Switch off 220V-Inverters
- Install auxiliary heating system on gravity meter or ship it

- Replace MYLINE by new line name, YYMMDDFFFF (Ultrasys: P, 1, xx, –9)
- Check serial output
    - 1 or 10 sec, long format (Ultrasys: C, 2, -8, -9, -9) 10
    - HighRes (Ultrasys: P, -9)

A.7 Fluxgate magnetometer specifications

Fluxgate magnetometer sensor [FG]

Range:	±70000nT
Resolution:	0.01nT
Accuracy:	0.4nT peak to peak at 8Hz
Sampling rate:	10Hz
Serial output:	10Hz RS232C
Range of thermometer:	-55C ~ +125C
Accuracy of thermometer:	0.1C

Data logger [SFG-2005]
The data logger boots up the FG sensor. After starting the FG sensor, the data logger sends these data to the PC for data backup and monitoring.

Ring Laser Gyro [RLG]
The attitude sensor is composed of three ring laser gyros and three single-axis accelerometers.

Table: Accuracy of output data

	Range	Resolution	Accuracy (24H)
Position	N90~S90, E180~W180	≤ 0.01 sec	5 NM
Velocity	-10Kt ~ +20Kt	≤ 0.08 knot	8 knot
Angular velocity	-10 ~ +10 / sec	≤ 0.01 / sec	0.05 /sec
Roll & Pitch angles	-90 ~ +90	≤ 0.025	0.05
Yaw angle	-180 ~ +180	≤ 0.025	0.5 / colatitude

Data format

The output data is recorded in the file named "Dyymmdd.txt" on the laptop. The characters of yy, mm and dd in the file name denote the last two figures of year, month and day of the recorded date in UTC, respectively. Examples of data strings are presented in Table 2, and the data format is as follows:

> Data number at every 10Hz, Year/ Month/ Day, Hour: Minute: Second, Latitude [degree], Longitude [degree], GPS fix (1) or not (0), Number of GPS, FG data [nT] Hx, Hy, Hz, FG temperature, *Gyro mode, Angular velocity [degree/sec] Roll, Pitch, Yaw, Angle [degree] Roll, Pitch, Azimuth, Velocity [m/sec] Vx, Vy, Vz, Latitude, Longitude, RLG data set

*Gyro Mode:
0: initial mode (until receive mode request)
1: alignment mode on land
2: alignment mode on ship
3: alignment mode on seabed
4: GPS hybrid mode
5: inertia mode
6: doppler hybrid mode (ground)
7: doppler hybrid mode (water)

Table: Examples of the output data

8, 2009/05/17, 13:52:19, -27.13412, 36.59892, 1, 7, 20314.15, 1498.64, -21743.15, 25.8, 0004, 0.024, -1.627, -0.003, 0.016, 2.098, -10.629, 2.6044, 0.4901, -0.1343, -27.13411, 36.59890, 00040008?=>;????0003017>?87110:;0323??24><;463091:06:02;
9, 2009/05/17, 13:52:19, -27.13412, 36.59892, 1, 7, 20274.47, 1507.43, -21764.87, 25.8, 0004, 0.064, -1.871, 0.049, 0.022, 1.917, -10.624, 2.6221, 0.5194, -0.0726, -27.13410, 36.59890, 00040015?=9;00100004015=?87210<80353??89><;463261:06:02<
0, 2009/05/17, 13:52:20, -27.13410, 36.59892, 1, 7, 20134.57, 1513.26, -21861.63, 25.8, 0004, 0.159, -2.191, -0.110, 0.033, 1.703, -10.629, 2.6440, 0.5530, -0.0098, -27.13410, 36.59890, 00040034?=32??=<00060136?87110><038:???0><;463431:06:02<

A.8 Information on the calibration circles

No.	Data	Time (UTC)	Latitude	Longitude
1	2009.04.15	08:42 - 10:34	-30.0004°	36.2023°
*2	2009.04.22	13:53 - 14:45	-34.3661°	33.4437°
3	2009.05.07	12:17 - 13:06	-29.8843°	31.5406°
4	2009.05.22	01:55 ~ 02:48	-27.1029°	33.7504°
5	2009.05.27	19:20 ~ 20:10	**-27.71°**	**34.33°**
6	2009.05.28	12:05 ~ 12:54	**-25.50°**	**34.14°**
7	2009.05.31	04:55 ~ 05:55	**-29.75°**	**32.00°**

** Results from AWI group's magnetic data, we identified that this area has very large variation of magnetic anomaly. Therefore, 2nd data will be excluded for the calibration of ship's magnetic field.*

- *The erroneous position data indicated by gray scale will be corrected from R/V Pelagia's GPS data after the cruise (please refer the term 4 and appendix A.5).*

A.9 File list of the shipboard three-component magnetometer data

<table>
<tr><th>Name</th><th>Size (MB)</th><th>data</th><th>Start (UTC)</th><th>End (UTC)</th><th>Note 1: status</th></tr>
<tr><td>D090409</td><td>89.8</td><td>2009.4.9</td><td>13:30:01</td><td>23:59:59</td><td>leg 1 departure 05:15

a few seconds of missing data occurred every 10 seconds.</td></tr>
<tr><td rowspan="2">D090410</td><td>163.4</td><td>2009.4.10</td><td>0:00:00</td><td>23:59:56</td><td>a few seconds of missing data occurred every 10 seconds.</td></tr>
<tr><td colspan="5">crane for CTD makes magnetic noise during 7:50 - 09:55</td></tr>
<tr><td>D090411</td><td>119</td><td>2009.4.11</td><td>0:00:00</td><td>23:59:59</td><td rowspan="5">a few seconds of missing data occurred every 10 seconds.</td></tr>
<tr><td>D090412</td><td>121.3</td><td>2009.4.12</td><td>0:00:00</td><td>23:59:56</td></tr>
<tr><td>D090413</td><td>125.5</td><td>2009.4.13</td><td>0:00:00</td><td>23:59:59</td></tr>
<tr><td>D090414</td><td>121.6</td><td>2009.4.14</td><td>0:00:00</td><td>23:59:59</td></tr>
<tr><td rowspan="2">D090415</td><td>129.2</td><td>2009.4.15</td><td>0:00:03</td><td>23:59:58</td></tr>
<tr><td colspan="5">figure 8 turn No. 1: 08:42 - 10:34</td></tr>
<tr><td>D090417</td><td>205.2</td><td>2009.4.17</td><td>0:00:00</td><td>23:59:59</td><td>a few seconds of missing data occurred every 10 seconds.</td></tr>
<tr><td>D090418</td><td>205.2</td><td>2009.4.18</td><td>0:00:00</td><td>23:59:59</td><td rowspan="5"></td></tr>
<tr><td>D090419</td><td>205.2</td><td>2009.4.19</td><td>0:00:00</td><td>23:59:59</td></tr>
<tr><td>D090420</td><td>205.2</td><td>2009.4.20</td><td>0:00:00</td><td>23:59:59</td></tr>
<tr><td>D090421</td><td>205.2</td><td>2009.4.21</td><td>0:00:00</td><td>23:59:59</td></tr>
<tr><td rowspan="3">D090422</td><td>205.2</td><td>2009.4.22</td><td>0:00:00</td><td>23:59:59</td></tr>
<tr><td colspan="5">dredging 05:00 - 13:40, figure 8 turn No. 2: 13:53 - 14:45</td></tr>
<tr><td colspan="5">crane for CTD makes magnetic noise during 16:40 - 19:10</td></tr>
<tr><td>D090423</td><td>205.2</td><td>2009.4.23</td><td>0:00:00</td><td>23:59:59</td><td rowspan="7"></td></tr>
<tr><td>D090424</td><td>205.2</td><td>2009.4.24</td><td>0:00:00</td><td>23:59:59</td></tr>
<tr><td>D090425</td><td>205.2</td><td>2009.4.25</td><td>0:00:00</td><td>23:59:59</td></tr>
<tr><td>D090426</td><td>205.2</td><td>2009.4.26</td><td>0:00:00</td><td>23:59:59</td></tr>
<tr><td>D090427</td><td>205.2</td><td>2009.4.27</td><td>0:00:00</td><td>23:59:59</td></tr>
<tr><td>D090428</td><td>205.2</td><td>2009.4.28</td><td>0:00:00</td><td>23:59:59</td></tr>
<tr><td>D090429</td><td>205.2</td><td>2009.4.29</td><td>0:00:00</td><td>23:59:59</td></tr>
<tr><td>D090430</td><td>205.2</td><td>2009.4.30</td><td>0:00:00</td><td>23:59:59</td><td rowspan="6">erroneous position data appeared.</td></tr>
<tr><td>D090501</td><td>205.1</td><td>2009.5.1</td><td>0:00:00</td><td>23:59:59</td></tr>
<tr><td>D090502</td><td>205.2</td><td>2009.5.2</td><td>0:00:00</td><td>23:59:59</td></tr>
<tr><td>D090503</td><td>205.2</td><td>2009.5.3</td><td>0:00:00</td><td>23:59:59</td></tr>
<tr><td>D090504</td><td>205.2</td><td>2009.5.4</td><td>0:00:00</td><td>23:59:59</td></tr>
<tr><td>D090505</td><td>205.1</td><td>2009.5.5</td><td>0:00:00</td><td>23:59:59</td></tr>
<tr><td rowspan="4">D090506</td><td rowspan="2">53.8</td><td rowspan="2">2009.5.6</td><td>0:00:00</td><td>6:12:31</td><td>erroneous position data appeared.</td></tr>
<tr><td>6:15:25</td><td>6:20:48</td><td>port-stop</td></tr>
<tr><td colspan="5">computer shut down 06:12:31</td></tr>
<tr><td colspan="5">*computer re-start for status check 06:15:25, system shut down 06:20:48</td></tr>
</table>

Name	Size (MB)	data	Start (UTC)	End (UTC)	Note 1: status
D090507	143	2009.5.7	7:12:08	7:12:38	erroneous position data appeared.
			7:16:50	23:59:59	leg 2 departure 08:53 erroneous position data appeared.
	*system re-start 07:12:08, system shut down for check connection 07:16:50				
	system re-start 07:16:50				
	figure 8 turn No. 3: 12:17 - 13:06				
D090508	205.1	2009.5.8	0:00:00	23:59:59	erroneous position data appeared.
D090509	205.2	2009.5.9	0:00:00	23:59:59	
D090510	205.2	2009.5.10	0:00:00	23:59:59	
D090511	205.2	2009.5.11	0:00:00	23:59:59	
D090512	205.2	2009.5.12	0:00:00	23:59:59	
D090513	205.2	2009.5.13	0:00:00	23:59:59	
D090514	205.2	2009.5.14	0:00:00	23:59:59	
D090515	205.2	2009.5.15	0:00:00	23:59:59	
D090516	205.2	2009.5.16	0:00:00	23:59:59	
D090517	205.1	2009.5.17	0:00:00	23:59:59	
D090518	205.2	2009.5.18	0:00:00	23:59:59	
D090519	205.2	2009.5.19	0:00:00	23:59:59	
D090520	205.2	2009.5.20	0:00:00	23:59:59	
D090521	205.1	2009.5.21	0:00:00	23:59:59	
D090522	205.2	2009.5.22	0:00:00	23:59:59	
	figure 8 turn No.4: 01:55 - 02:48				
D090523	205.2	2009.5.23	0:00:00	23:59:59	
D090524	205.1	2009.5.24	0:00:00	23:59:59	
D090525	205.2	2009.5.25	0:00:00	23:59:59	erroneous position data appeared.
	dredging 06:30 - 00:10				
D090526	205.2	2009.5.26	0:00:00	23:59:59	erroneous position data appeared.
D090527	205.2	2009.5.27	0:00:00	23:59:59	
	figure 8 turn No.5: 19:20 - 21:10				
	crane for CTD make magnetic noise during 17:50 - 19:10				
D090528	205.1	2009.5.28	0:00:00	23:59:59	erroneous position data appeared.
	figure 8 turn No.6: 12:05 - 12:54				
D090529	203.6	2009.5.29	0:00:00	19:10:34	erroneous position data appeared.
			19:21:27	23:59:59	
	all systems shut down because of plug fall out 19:10				
	system re-start 19:21:27, and RLG alignment is finished 20:09:37				
D090530	205.2	2009.5.30	0:00:00	23:59:59	erroneous position data appeared.
D090531	72.8	2009.5.31	0:00:00	8:30:52	erroneous position data appeared. return to port
	Figure 8 turn No.7: 04:55 - 5:55				
	stop all systems 08:30:52				

Die "Berichte zur Polar- und Meeresforschung" (ISSN 1866-3192) werden beginnend mit dem Heft Nr. 569 (2008) ausschließlich elektronisch als Open-Access-Publikation herausgegeben. Ein Verzeichnis aller Hefte einschließlich der Druckausgaben (Heft 377-568) sowie der früheren **"Berichte zur Polarforschung** (Heft 1-376, von 1982 bis 2000) befindet sich im Internet in der Ablage des electronic Information Center des AWI (**ePIC**) unter der URL http://epic.awi.de. Durch Auswahl "Reports on Polar- and Marine Research" auf der rechten Seite des Fensters wird eine Liste der Publikationen in alphabetischer Reihenfolge (nach Autoren) innerhalb der absteigenden chronologischen Reihenfolge der Jahrgänge erzeugt.

To generate a list of all Reports past issues, use the following URL: http://epic.awi.de and select the right frame to browse "Reports on Polar and Marine Research". A chronological list in declining order, author names alphabetical, will be produced, and pdf-icons shown for open access download.

Verzeichnis der zuletzt erschienenen Hefte:

Heft-Nr. 585/2009 — "Population dynamics of the surf clams *Donax hanleyanus* and *Mesodesma mactroides* from open-Atlantic beaches off Argentina", by Marko Herrmann

Heft-Nr. 586/2009 — "The Expedition of the Research Vessel 'Polarstern' to the Antarctic in 2006 (ANT-XXIII/7)", edited by Peter Lemke

Heft-Nr. 587/2009 — "The Expedition of the Research Vessel 'Maria S. Merian' to the Davis Strait and Baffin Bay in 2008 (MSM09/3), edited by Karsten Gohl, Bernd Schreckenberger, and Thomas Funck

Heft-Nr. 588/2009 — "Selected Contributions on Results of Climate Research in East Germany (the former GDR)", edited by Peter Hupfer and Klaus Dethloff

Heft-Nr. 589/2009 — "The Expedition of the Research Vessel 'Polarstern' to the Arctic in 2008 (ARK-XXIII/1)", edited by Gereon Budéus

Heft-Nr. 590/2009 — "The Expedition of the Research Vessel 'Polarstern' to the Arctic in 2008 (ARK-XXIII/2)", edited by Gerhard Kattner

Heft-Nr. 591/2009 — "The Expedition of the Research Vessel 'Polarstern' to the Antarctic in 2008 (ANT-XXIV/4)", edited by Andreas Macke

Heft-Nr. 592/2009 — "The Expedition of the Research Vessel 'Polarstern' to the Antarctic in 2007 (ANT-XXIV/1)", edited by Sigrid Schiel

Heft-Nr. 593/2009 — "The Campaign MELTEX with Research Aircraft 'POLAR 5' in the Arctic in 2008", edited by Gerit Birnbaum, Wolfgang Dierking, Jörg Hartmann, Christof Lüpkes, André Ehrlich, Thomas Garbrecht, and Manuel Sellmann

Heft-Nr. 594/2009 — "The Expedition of the Research Vessel 'Polarstern' to the Antarctic in 2008 (ANT-XXV/1)", edited by Gerhard Kattner and Boris Koch

Heft-Nr. 595/2009 — "The Expedition of the Research Vessel 'Polarstern' to the Antarctic in 2008/2009 (ANT-XXV/2)", edited by Olaf Boebel

Heft-Nr. 596/2009 — "Crustal evolution of the submarine plateaux of New Zealand and their tectonic reconstruction based on crustal balancing", by Jan Werner Gerhard Grobys

Heft-Nr. 597/2009 — "The Expedition of the Research Vessel 'Polarstern' to the Arctic in 2008 (ARK-XXIII/3)", edited by Wilfried Jokat

Heft-Nr. 598/2009 — "The Expedition of the Research Vessel 'Pelagia' to the Natal Basin and the Mozambique Ridge in 2009 (Project AISTEK III)", edited by Wilfried Jokat